A NEW PRECIPITATION RECYCLING MODEL

A Thesis
Presented to
The Academic Faculty

by

Minjae Kim

In Partial Fulfillment
of the Requirements for the Degree
Mater of Science in
Civil and Environmental Engineering

Georgia Institute of Technology
May 2018

A NEW PRECIPITATION RECYCLING MODEL

Approved by:

Dr. Jingfeng Wang, Advisor
School of Civil and Environmental Engineering
Georgia Institute of Technology

Dr. Jian Luo
School of Civil and Environmental Engineering
Georgia Institute of Technology

Dr. Yi Deng
School of Earth and Atmospheric Sciences
Georgia Institute of Technology

Date Approved: January 12, 2018

ACKNOWLEDGEMENTS

First and most of all, I appreciate to Dr. Jingfeng Wang for his expertise, instruction, and guidance through of this thesis work. He gave me the way for better understanding of my study and inspired me to finish this study well. And I also appreciate my committee members, Dr. Jian Luo and Dr. Yi Deng for their support and encouragement.

I would like to extend my gratitude to colleague graduate student Yao Tang for many generous and helpful suggestions.

TABLE OF CONTENTS

LIST OF TABLES

LIST OF FIGURES

LIST OF SYMBOLS AND ABBREVIATIONS

α	Parameter for a new model, mixing index
AD	Advection Dominant
CV	Control Volume
E	Evaporation
F_q	Water vapor flux
GMC	Global Climate Model
GPM	Global Precipitation measurement
LED	Local Evaporation Dominant
NCEP	National Center for Environmental Prediction
P	Precipitation
PACE	partnership for an Advanced Computing Environment
PRC	Precipitation recycling
q	Specific Humidity
ρ	Precipitation Recycling ratio
RCM	Regional Climate Model
TRMM	Tropical Rainfall Measurement Mission
USGS	United States Geological Survey
w	Precipitable water
V	Wind vector

SUMMARY

The purpose of this study is to formulate and test a new model of precipitation recycling ratio. Precipitation recycling ratio is a diagnostic variable defined as the ratio of precipitation from local evaporation to the total precipitation over a given area of concern. A new model of precipitation recycling ratio is formulated based on not well-mixed assumption as a generalization of the conventional models developed based on the well-mixed assumption. An empirical parameter α was introduced to represent the not well-mixed condition. This study proposed possible physical mechanisms corresponding to the not well-mixed assumption. Numerical simulations of the precipitation recycling ratio were conducted under various conditions such as change of α, evaporation, and precipitation which are major variables in the new model. The used data sets were retrieved from National Centers for Environmental Prediction (NCEP) over the South America for period of 1993 to 2006. Using the reanalysis data of evaporation, precipitation, simulations were performed to understand effects of α, evaporation and precipitation to the precipitation recycling ratio. Precipitation has negative contribution to precipitation recycling ratio under local evaporation dominant condition, while it has positive contribution to precipitation recycling ratio under advection dominant condition. It was found that the distribution of precipitation recycling ratio was influenced by topography such as Mountains Andes, advection of water vapors, and extreme climate events such as El Nino. This study suggests an application of new data set and expansion of study domain to global scale.

1. Introduction

1.1 Precipitation recycling

Precipitation refers to condensed water released from cloud in many forms such as rain, snow or hail, sleet, freezing rain as defined by United States Geological Survey (USGS). Precipitation originates from land and ocean evaporation into the atmosphere. Precipitation at a certain location in a given domain comes from evaporated water vapor within the domain or from outside through advection. Here we ask the question: what is the ratio of precipitation water coming from evaporation within a given region to that from advection into the domain?

Precipitation recycling is defined as the contribution of local evaporation within a region to precipitation over the same region. Precipitation recycling ratio is the ratio of precipitation from local evaporation to total precipitation falling at the domain (Eltahir and Bras 1994). Precipitation recycling ratio ranges from zero to one with zero indicating no local evaporation within the region, and one meaning all precipitation coming from evaporation within the region.

1.2 Land-use and precipitation

An old phrase, “Rain follows the plow”, suggests that land-use and land cover change may influence precipitation. Generally, land-use affects the surface water balance and evaporation which would influence precipitation. For example, the Tocatins river basin in Brazil showed up to 25% increase in river discharge between 1960 and 1995 after deforestation while no significant change in precipitation during that period.(Costa, Botta et al. 2003) Human activities such as dam construction and deforestation which induced impact of land cover change on surface hydrology are well documented by many researchers. Precipitation recycling ratio as a diagnostic variable quantitatively characterizes certain relationship between surface hydrology

and regional climate. Higher recycling ratio means a greater fraction of water vapor comes from local evaporation implying a stronger hydrologic cycle. On the other hand, smaller ratio means a greater fraction of precipitation is advected into the region by the atmospheric circulations. Therefore, the recycling ratio is a measure of the intensity of land-atmosphere interaction. van der Ent et al (2010) argued that ”the magnitude of moisture recycling can be used as an indicator for the sensitivity of climate to land-used change’’(van der Ent, Savenije et al. 2010) Precipitation recycling ratio helps further understanding of the interaction between precipitation and land surface hydrology.

1.3 Modeling Precipitation Recycling Ratio

There are three types of methods for modeling precipitation recycling ratio.

The first method is based on the stable isotope of water. To separate local evaporation source from advection source, Salati et al applied the isotope method for computation of precipitation recycling (Salati, Dall'Olio et al. 1979). In their study, monthly samples of precipitation and river water were collected in 1972 at representative sites throughout the Amazon basin. Precipitation recycling ratio was calculated from the measurements of water isotopes. Kurita et al collected isotope data at 13 stations across Russia from 1996 to 2000. They found that in Siberia more than half of the summer precipitation originated from local evaporation (Kurita, Yoshida et al. 2004). This method connects directly precipitation recycling and real physical water vapor.

The second method is numerical simulation. Precipitation recycling ratio is simulated using Global Climate Model (GCM) or Regional Climate Model (RCM). Three types of techniques are adopted in the numerical simulation method: (1) simulation of precipitation with and without (potential) evaporation, (2) tracking moisture sink and sources over multiple regions, (3) adding

isotopes in water as passive tracers. In the 1980s, Shukla and Mintz (1982) applied the first method to study the global precipitation recycling.(SHUKLA and MINTZ 1982) Although they did not explicitly trace the origins of land surface precipitation, their result supported the possibility of application of GCM in precipitation recycling analysis. The second method based on the concept of tracking moisture in numerical models is widely accepted for studying precipitation recycling on regional, continental, and global scales (Koster, Jouzel et al. 1992, Koster, de Valpine et al. 1993, Numaguti 1999, Delaygue, Masson et al. 2000, Yoshimura, Oki et al. 2004, Risi, Noone et al. 2013). Although the numerical modeling using GCMs is computationally more efficient, the model simulations have large uncertainties due to the variability of isotopes. Another limitation of numerical models is that the GCM simulations are subject to modeling errors of parameterizations of physical processes in the GCM's.

The third method is based on two physical concepts: 1) the conservation of atmospheric water vapor using the Eulerian approach, or 2) calculation of the trajectory of water vapor using the Lagrangian approach. Based on the first concept, Budyko and Drizdiv (1953) first developed a simple one-dimensional formula expressing the recycling ratio as a function of evaporation, horizontal water vapor influx, and the length of the region (Burde and Zangvil 2001). Budyko's model presents precipitation recycling along with a single streamline. It was assumed that the spatial distributions of evaporation and precipitation are the same. In some studies, afterward, Brubaker et al. (1993) generalized the one-dimensional model to a two-dimensional one. (Brubaker, Entekhabi et al. 1993). Trenberth (1999) and Bosilovich and Schubert (2002) adopted the two-dimensional model of Brubaker.(Bosilovich, Sud et al. 2003) In the two-dimensional Eulerian model, variables such as vertical fluxes, precipitation, and evaporation were taken as constant values. Without assuming horizontal homogeneity, Eltahir and Bras (1994; 1996)

proposed a general formula to estimate the precipitation recycling ratio. This general formula was derived based on two assumptions: 1) water vapor is well mixed in the atmospheric boundary layer, and 2) the change rate of water vapor storage is negligible compared to water vapor flux at the time-scale for which their recycling model is applicable. This general formula was widely applied to study precipitation recycling processes (Bosilovich and Schubert 2001; Fitzmaurice 2007; Guihua 2013). In all previous theoretical models, precipitation recycling was parametrized as function of horizontal atmospheric fluxes, evaporation, and precipitation. Savenije (1995) further considered other hydrological parameters such as infiltration and runoff using a one-dimensional moisture recycling model for studying the relationship between land-use and climate over the Sahel (Savenije 1995).

1.4 Well-mixed assumption

Well-mixed assumption plays a key role in the existing models of precipitation recycling (Eltahir and Bras 1994). Water vapor being well-mixed in the planetary boundary layer implies that water molecules of external (advection) origin and those of internal (evaporative) origin have equal probabilities to precipitate (Burde 2006). Hence, the ratio of moisture (specific humidity) q_m originated from local evaporation to total precipitable water q is equal to that of locally originated precipitation P_m and total precipitation P. Then precipitation recycling ratio ρ is:

$$\rho = \frac{q_m}{q} = \frac{P_m}{P} \quad (1)$$

The well-mixed assumption is based on the argument that all water vapor molecules within the vertical column of the atmosphere have the same chance to be condensed out as rain. In this analysis, we investigate the general cases of non-well-mixed atmospheric boundary layer.

1.5 Thesis Outline

This study is motivated by seeking answers to the following three questions. First, whether the well-mixed assumption is universal? Second, if the well-mixed condition is not universal, what are the physical conditions representing the not well-mixed assumption? Third, how do the not well-mixed conditions affect precipitation recycling ratio?

This study consists of three parts. Part one provides a general discussion on the well-mixed vs. not well-mixed assumption. Part two presents the formulation of the new model of precipitation recycling ratio based on the not well-mixed condition and numerical simulations of recycling ratio of the South America continent. The effects of mixing index α, local evaporation, precipitation and advective water vapor on the distribution of precipitation recycling ratio were evaluated. Part three discusses the test results and possible physical mechanisms behind the not well-mixed conditions.

2. Theory

2.1. An overview of well mixed model of precipitation recycling

The overview of the well-mixed model follows the work of Eltahir and Bras (1994). For a control volume (CV) as shown in Figure 1 below, there are three mass fluxes of water vapor: inflow and outflow through advection, local evaporation and precipitation.

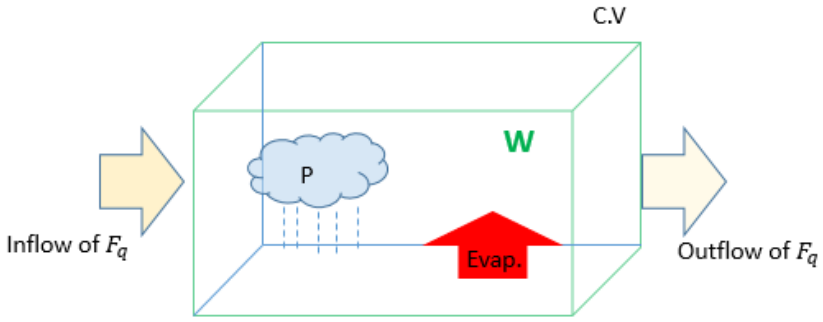

Figure 1. Simplified water balance

The water balance equation for the control volume (CV) is expressed in terms of change of water vapor storage (precipitable water) equals to the net water fluxes. Precipitable water w is the total water vapor within the entire column of atmosphere expressed as the vertical integral of specific humidity q from the surface to the top of the atmosphere where atmospheric pressure p vanishes when using pressure as the vertical coordinate,

$$w = \int_0^{p_s} q(p)\frac{dp}{g} \tag{2}$$

where Ps is the surface pressure. Horizontal advective water vapor flux $\overrightarrow{F_q}$ is represented by the vertical integral of specific humidity q multiplied by the horizontal wind velocity $\vec{V}$,

$$\vec{F}_q = \int_0^{P_s} \vec{V}(p)q(p)\frac{dp}{g} \tag{3}$$

w consists of water vapor from advection w_a and that from local evaporation w_m,

$$w=w_a+w_m \tag{4}$$

Likewise, q has two components associated with advection and local evaporation, respectively,

$$q=q_a+q_m \tag{5}$$

The water balance equation for the CV is,

$$\frac{\partial w}{\partial t}+\nabla\cdot\vec{F}_q=E-P \tag{7}$$

where $\nabla\equiv\left(\frac{\partial}{\partial x},\frac{\partial}{\partial y}\right)$ and x,y the horizontal coordinates.

Then,

$$\frac{\partial w_m}{\partial t}+\nabla\cdot\vec{F}_{qm}=E-P_m \tag{8}$$

Under the well-mixed equation, variables such as w_m and F_{qm} or local component of F_q can be expressed as below.

$$w_m=\int_0^{P_s} q_m\frac{dP}{g}=\rho w \tag{9}$$

$$\vec{F}_{q_m}=\int_0^{P_s}\overrightarrow{V_m}\,q_m\frac{dP}{g}=\rho\vec{F}_q \tag{10}$$

Combining (8), (9) and (10) leads to,

$$\frac{\partial w_m}{\partial t}+\nabla\cdot\vec{F}_{qm}=\frac{\partial \rho w}{\partial t}+\nabla\cdot(\rho\vec{F}_{qm})=E-\rho P$$

$$\rho\frac{\partial w}{\partial t}+w\frac{\partial \rho}{\partial t}+\rho\nabla\cdot\vec{F}_q+\vec{F}_q\cdot\nabla\rho=E-\rho P$$

$$\rho\left(\frac{\partial w}{\partial t}+\nabla\cdot\vec{F}_q\right)+w\frac{\partial \rho}{\partial t}+\vec{F}_q\cdot\nabla\rho=E-\rho P$$

$$\rho(E-P)+w\frac{\partial \rho}{\partial t}+\vec{F}_q\cdot\nabla\rho=E-\rho P$$

$$w\frac{\partial \rho}{\partial t}+\vec{F}_q\cdot\nabla\rho=(1-\rho)E \qquad (11)$$

Equation (11) is the governing equation of the recycling ratio ρ. The boundary condition of ρ at inflow boundary is zero since there is no local source of water vapor from evaporation.

2.2 Not well-mixed assumption or inhomogeneity

Some researchers question the validity of the well-mixed assumption. Fast recycling was suggested as one of the reasons that the well-mixed assumption does not hold (Lettau, Lettau et al. 1979). Fast-recycling is a process that local convective precipitation forms before cloud water vapor of local and advective sources completely mixed. Fast recycling implies that water vapor of local and advection origin would not have the same probabilities of being condensed into precipitation.

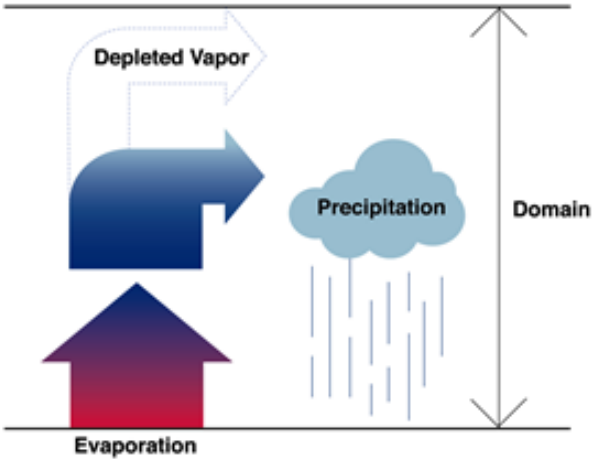

Figure 2 Fast recycling. The water vapor from evaporation is recycled in a 'fast' way

In a study of vertical distribution of water vapor, Bosilovich (2002) found moisture mixing ratio (local vs. advective origin) tends to be non-uniformly distributed vertically with more moisture of local origin being higher at lower levels. Goessling and Reick (2013) suggested that the vertical inhomogeneities of moisture origin may be caused by localized evaporation and directional wind shear.(Goessling and Reick 2013) Evaporation increases moisture of local origin in the lower part of the atmosphere that invalidates the well-mixed assumption due to the sudden increase of moisture from local origin. They tested quantitatively the validity of well-mixed assumption by comparing the 2D and 3D model of moisture tracking. If the atmospheric moisture is well-mixed vertically, the 2-D approximation is exact. But they found that the 2D water vapor tracking (WVT) is different from the 3D WVT for certain regions such as Sahel. Previous quantitative analyses suggest that the well-mixed assumption would not be universally hold. In this study, we formulated a revised to solve the well-mixed problem.

2.3 Formulation of not-well-mixed model

2.3.1 Parameterization of not-well-mixed assumption in precipitation recycling model (PRC).

One parameterization of the not-well mixed assumption is to include a linear in equations (1) as following,

$$\rho = \alpha \frac{q_m}{q} = \frac{P_m}{P} \tag{12}$$

where α is ranged from zero to one. Plugging in equation (12) into equation (7) then, it will generate a modified governing equation, as

$$\frac{d\rho}{dt} + \frac{1}{w}\vec{F}_q \cdot \nabla\rho = (\alpha - \rho)\frac{E}{w} + (1-\alpha)\rho\frac{P}{w} = \left[(1-\alpha)\frac{P}{w} - \frac{E}{w}\right]\rho + \alpha\frac{E}{w} \tag{13}$$

A problem of equation (13) can be found when it is derivatized numerically and the justification is expressed in Appendix A. Because equation (13) does not work well with boundary conditions, so equation (12) will be ruled out. Here we propose a new parameterization,

$$\rho = (\frac{q_m}{q})^{\alpha} = \frac{P_m}{P} \tag{14}$$

Where α is greater than zero. Substituting equation (14) into equation (7) leads to,

$$P_m = \rho P$$

$$q_m = \rho^{\frac{1}{\alpha}} q$$

$$w_m = \rho^{\frac{1}{\alpha}} w$$

$$\vec{F}_{qm} = \rho^{\frac{1}{\alpha}} \vec{F}_q$$

The new governing equation under not-well mixed assumption can be derived as,

$$\frac{\partial \rho^{\frac{1}{\alpha}} w}{\partial t} + \nabla \rho^{\frac{1}{\alpha}} \cdot \vec{F}_q = E - \rho P$$

$$\rho^{\frac{1}{\alpha}} \frac{\partial w}{\partial t} + w \frac{\partial \rho^{\frac{1}{\alpha}}}{\partial t} + \rho^{\frac{1}{\alpha}} \cdot \nabla \vec{F}_q + \vec{F}_q \cdot \nabla \rho^{\frac{1}{\alpha}} = E - \rho P$$

$$\rho^{\frac{1}{\alpha}} \left(\frac{\partial w}{\partial t} + \nabla \cdot \vec{F}_q \right) + w \frac{\partial \rho^{\frac{1}{\alpha}}}{\partial t} + \vec{F}_q \cdot \nabla \rho^{\frac{1}{\alpha}} = E - \rho P$$

$$\frac{\partial \rho^{\frac{1}{\alpha}}}{\partial t} + \frac{\vec{F}_q}{w} \cdot \nabla \rho^{\frac{1}{\alpha}} = (1 - \rho^{\frac{1}{\alpha}}) \frac{E}{w} - (\rho - \rho^{\frac{1}{\alpha}}) \frac{P}{w}$$

$$\frac{\partial \rho}{\partial t} + \frac{\vec{F}_q}{w} \cdot \nabla \rho = \alpha \left(\rho^{1-\frac{1}{\alpha}} - \rho \right) \frac{E}{w} - \alpha \left(\rho^{2-\frac{1}{\alpha}} - \rho \right) \frac{P}{w} \qquad (15)$$

Then using method of characteristic, equation (16) may be re-written as,

$$\begin{cases} dx = \dfrac{F_{q_x}}{w} dt \\ dy = \dfrac{F_{q_y}}{w} dt \\ d\rho = \alpha \left(\rho^{1-\frac{1}{\alpha}} - \rho \right) \dfrac{E}{w} - \alpha \left(\rho^{2-\frac{1}{\alpha}} - \rho \right) \dfrac{P}{w} dt \end{cases}$$

According to the Euler method, ρ can be expressed as :

$$\rho_{i+1} = \rho_i + \left[\alpha \left(\rho_i^{1-\beta} - \rho_i \right) \frac{E}{w} - \alpha \left(\rho_i^{2-\beta} - \rho_i \right) \frac{P}{w} \right] h \qquad (16)$$

where h is the time step. Given the boundary condition ρ_1 is equal to zero at the inflow boundary, the time evolution of ρ over the domain can be obtained by numerically integrating equation (16). Using Runge-Kutta method. (The FORTLAN code provided by Dr. Wang was modified by Yao Tang of Georgia Institute of Technology) its numerical expression is shown in Appendix B. If we set $\frac{1}{\alpha}$ as β, Equation (16) is expressed as below.

$$\frac{\partial \rho}{\partial t} + \frac{\vec{F}_q}{w} \cdot \nabla \rho = \alpha \left(\rho^{1-\beta} - \rho \right) \frac{E}{w} - \alpha \left(\rho^{2-\beta} - \rho \right) \frac{P}{w}$$

2.3.2 Determination of range of parameter α

The empirical coefficient α in equation (16) has physical meanings as indicated in Table 1

$$\frac{\partial \rho}{\partial t} + \frac{\vec{F}_q}{w} \cdot \nabla \rho = \alpha \left(\rho^{1-\frac{1}{\alpha}} - \rho \right) \frac{E}{w} - \alpha \left(\rho^{2-\frac{1}{\alpha}} - \rho \right) \frac{P}{w}$$

Table 1. Definitions for α value ranges and corresponding physical conditions

α	Definition	Physical condition
< 1	Sub-well-mixed	Evaporation is the only source for precipitation
1	Well-mixed	Well-mixed condition
> 1	Super-well-mixed	No evaporation, advection is the only source for precipitation

There are three cases in the Table 1. When α is greater than one, it represents the advection dominant condition. While α is less than one, this represents local evaporation-dominant condition. When α approaches zero, the recycling ratio to one, implying no advective water vapor contributing to precipitation (imaging that evaporation occurs in a closed box). When α approaches infinity, the recycling ratio becomes zero, implying that local evaporation has no contribution to precipitation and the advective water vapor is the only source of precipitation. This situation is similar to precipitation over desert regions. Figure 3 below demonstrates the two limiting cases.

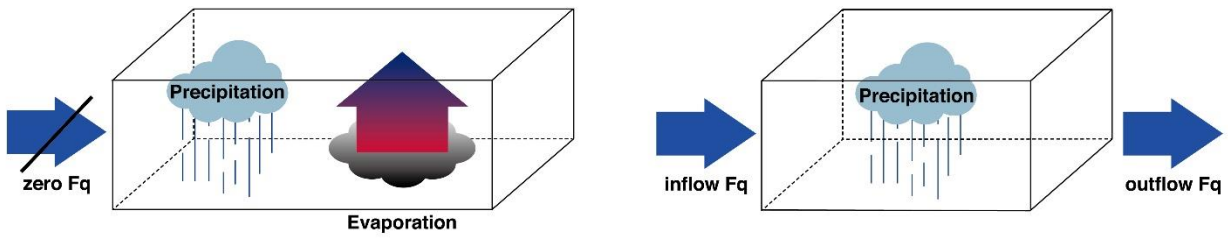

Figure 3 A physical situation describing when α is equal to zero (Left). A case with α as infinite value (Right). If α is zero, advection would be zero. But if α becomes infinite value, that means there is no evaporation.

Both of previous descriptions are discussed in the context of evaporation and advection. Secion 2.1.1, the not well-mix condition was addressed with repsect to probability. The not well-mixed

conditions include two cases: α less than one means that water vapor from local evaporation has higher chance or higher probability to be condensed, and α greater than one means than water vapor from advection has more chance or higher probability to be condensed. Next, this study will report the sensitivity test to quantify the impact of α on the recycling ratio.

For the well-mixed case, the 2nd term on the right-hand-side (RHS) of equation (16) vanishes and precipitation has no influence on the recycling ratio. When α is equal to one, the 2nd term on the RHS of equation (16) becomes zero. When α is greater than one, the 1st term on the RHS of equation (16) is positive, while the 2nd term is negative. Advection (local evaporation) is more (less) important in term of water vapor resource when α increases (decreases). In this study, a case when α is smaller than one is referred to as local evaporation dominant (LED) condition. LED condition means that probability of water vapor condensation from local evaporation is greater than that of advection. Another case when α is greater than one is referred to as advection dominant (AD) condition. The AD condition means that probability of water vapor condensation from advection is greater than that of local evaporation. Numerical simulations of recycling ratio according to equation (16) will conducted for a range of α values.

2.4 Numerical simulations of the not well-mixed model

A series of sensitivity tests will be conducted to understand the influence of α on precipitation recycling ratio. The study domains are selected in the tropical and subtropical regions. In a tropical area, evaporation is stronger than that in a subtropical area. In contrast, advection is stronger in a tropical area than that in a subtropical area. Therefore, the well-mixed condition is more likely to prevail in tropical area than not-well-mixed condition. The study domains for sensitivity test are selected to be representative for well-mixed and not well-mixed

conditions. All numerical simulations run on the PACE system of Georgia Tech. The FORTRAN code was originally prepared by Dr. Wang, Jingfeng and revised by Yao Tang.

The tests of the not well-mixed model consist of four parts. The first part focuses on an understanding the impact of α on the governing equation (16) for various fixed values of recycling ratio ρ. The second part focuses on variability of ρ in response to a range of α values for a given year. The third part focuses on the inter-annual variability of ρ during 1992 to 2006. The fourth part investigates the sensitivity of the numerical simulations of recycling ratio to the data of evaporation and precipitation. The not well-mixed model needs precipitation data as an input while the well-mixed model as in equation (7) does not. That is a key point of the new model.

3. Data and Study Domain

National Center for Environmental Prediction (NCEP) infrared data is the primary data set for this study. (http://www.esrl.noaa.gov/psd/data/gridded/data.ncep.reanalysis.html). The data product provides wind speed, specific humidity, surface pressure, evaporation (latent heat fluxes) and land-sea mask. The 4-times daily data product has spatial coverage which is 2.5°×2.5° global grids (144×73) from 0.0° E to 357.5° E longitude and 90.0° N to 90.0° S latitude. Wind speed and specific humidity are on pressure levels from surface up to 300 mb containing approximately 99% of the atmospheric water vapor. Data of surface pressure and land-sea mask are obtained under the Surface Section of NECP. The spatial coverage of surface pressure and land-sea mask on surface level is the same as that on pressure level. The latent heat fluxes data on surface level are obtained under the Surface Flux Section. The spatial coverage of latent heat flux data on surface level is T62 Gaussian grid with 192×94 points from 88.542° N to 88.542° S and 0° E to 358.125° E. The latent heat flux data from NCEP IR are classified as category-"C", meaning the they are solely model simulations constrained only by the model states and parameterizations (Kalnay, Kanamitsu et al. 1996). There is no "ground truth" for latent heat flux data (Kistler, Collins et al. 2001), The uncertainty of latent heat flux over land used in this study is smaller than that over oceans (Trenberth and Guillemot 1998).

The study domain is the South America Continent. In the land mask in the NCEP data set, the coordinates of the four corners are [20° S, 260° E], [20° S, 340° E], [60° S, 340° E], [60° S, 260° E]. The figure below shows the topography of the South America.

Figure 4 South America Continent (PIA03388: South America, Shaded Relief and Colored Height by Shuttle Radar Topography Mission of NASA)

4. Results and Discussions

4.1 Effect of α on ρ

The coefficients of the first and second term on the RHS of equation (16), $\alpha\left(\rho^{1-\frac{1}{\alpha}}-\rho\right)\frac{E}{w}$, $-\alpha\left(\rho^{2-\frac{1}{\alpha}}-\rho\right)\frac{P}{w}$, are evaluated first to understand the effect of *a*, on recycling ratio ρ for given E (evaporation) and P (precipitation). as shown in Figure 5.

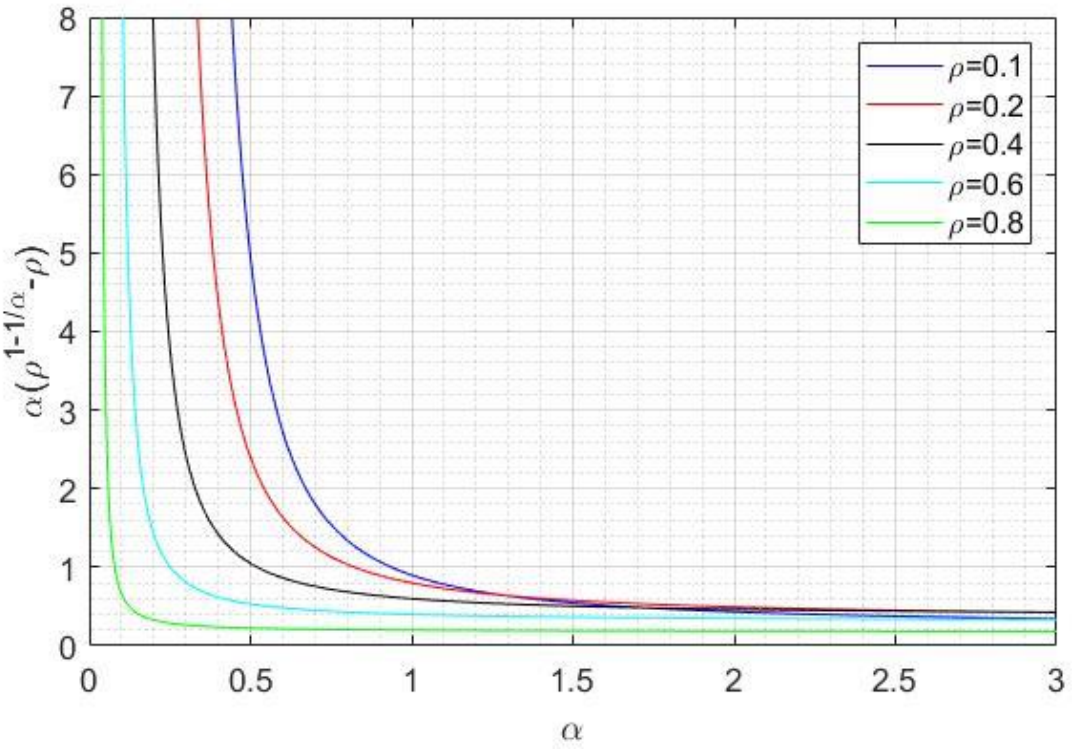

Figure 5 The first term of the governing equation vs. α for different ρ values. Each $\alpha\left(\rho^{1-\frac{1}{\alpha}}-\rho\right)\frac{E}{w}$ ***converges into different values***

The coefficient of the 2nd term on the RHS of equation (16) is shown in Figure 6.

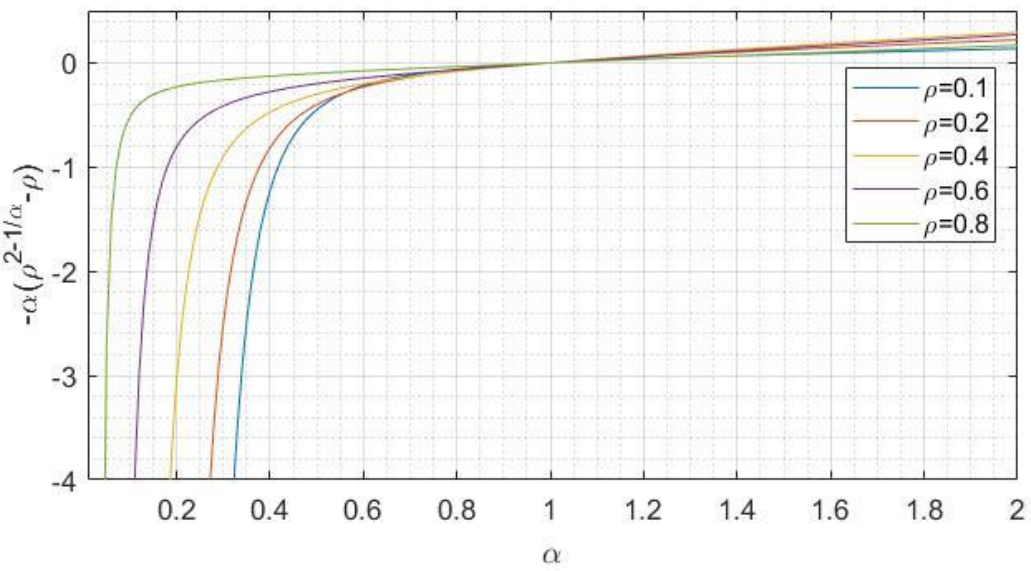

Figure 6 The second term of the governing equation vs. α with different ρ values. When α is greater than one, the sign of $-\alpha\left(\rho^{2-\frac{1}{\alpha}}-\rho\right)$ ***changes from negative to positive.***

In Figure.5, the first term with higher ρ value is smaller than that with smaller ρ. As ρ gets higher, the impact of the first term gets smaller. And the change of the first term over α becomes stabilized and the y values converges to certain values. If α becomes to infinite value, the 1st term except E converges to 0.2302, 0.3612, 0.3665, 0.3065, 0.1785 for ρ as 0.1, 0.2, 0.4, 0.6, 0.8 respectively. This shows that the effect of α to the governing equation is depending on size of α. In Figure 6, if α is close to zero (+0), the 2nd term becomes negative infinite. When α is greater than one, the second terms changes its sign. The effect of α on the coefficient of the second term is that the types of not well-mixed condition determine its sign. So, the effect α on the governing equation depends on the magnitude of α under both conditions. Figure 7 shows the changing of the second term under the AD condition. The second term appears to be nearly linear under AD condition as shown in Figure 7. In Figure 6, the second term with lower α has lower value than that with higher α under LED condition. α has no correlation with the second

term under AD condition as shown in Figure 7. The second term with α as 0.1 is smaller than that with α as 0.2, while the second term with α as 0.2 is greater than the second term with α as 0.8. The effect of α on the second term under LEP condition is different from the effect of α to the second term under AD condition.

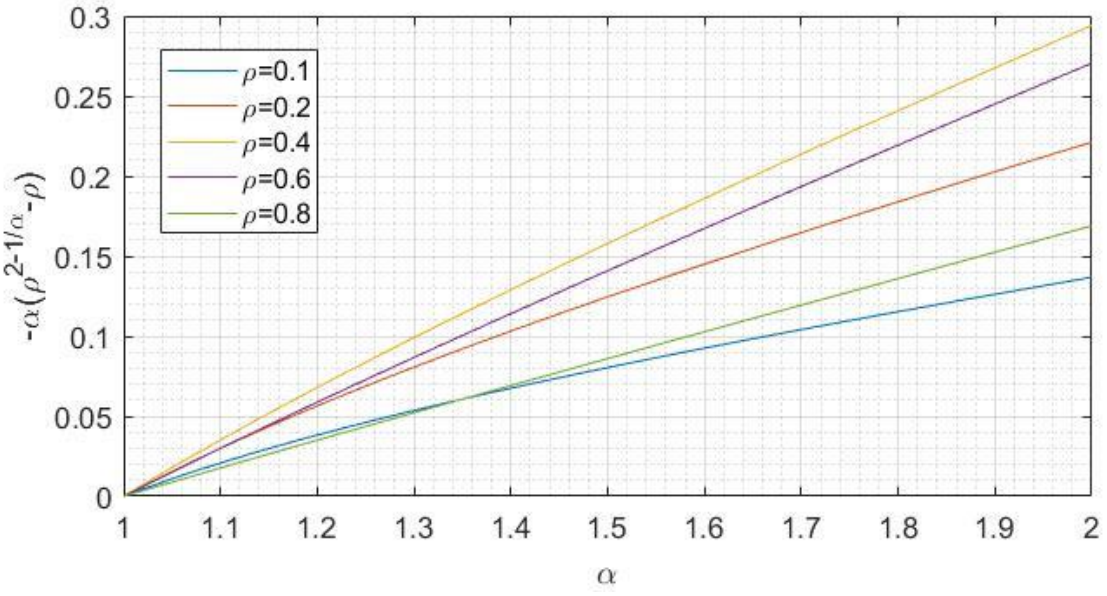

Figure 7 Linearity of the second term along a with given ρ. Under the AD condition, the shape of the $-\alpha\left(\rho^{2-\frac{1}{\alpha}}-\rho\right)$ ***becomes rather linear shape.***

4.2 Simulation of ρ for 2003

Using a numerical algorithm described in chapter 2, precipitation recycling ratio ρ with various α values were computed for 2003 of South America continent. Values of α ranging from 0 to 4000 were selected. The annual mean domain averaged ρ varying with α is shown in Figure 7. The numerical values are given in Table 2.

Table 2. Recycling ratio over various α of South America for 2003

α	ρ [%]	α	ρ [%]	α	ρ [%]	α	ρ [%]
0.01	75.3	0.9	29.4	1.9	20.4	100	9.8
0.1	66.7	1	27.2	2	20.0	200	9.7
0.2	57.7	1.1	26.4	3	17.3	400	9.7
0.3	50.3	1.2	25.2	5	14.9	700	9.7
0.4	44.6	1.3	24.2	7	13.7	1000	9.6
0.5	40.2	1.4	23.4	10	12.6	2000	9.5
0.6	36.6	1.5	22.6	20	11.2	4000	9.5
0.7	33.7	1.7	21.4	40	10.3		
0.8	31.4	1.8	21.8	80	9.9		

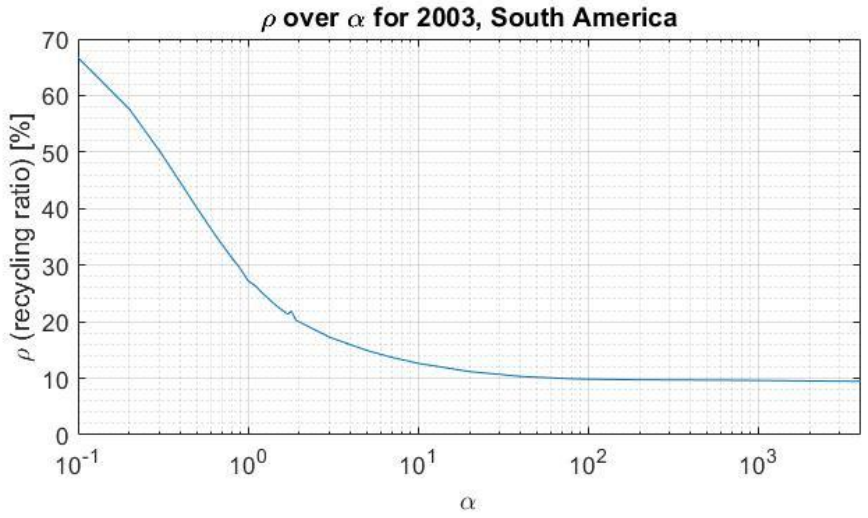

Figure 8 Annual mean domain averaged recycling ratio ρ, x-axis as log scaled α. Under LED condition, the change of ρ over α is drastic but the change becomes weaker under AD condition

ρ changes from 75% to 27% while α changes from 0.01 to 1. ρ changes from 27% to 20% when α changes from 1 to 2. Hence, the changes of ρ under evaporation dominant condition are greater than under advection dominant condition. To show the Figure 9 shows that the changes of ρ under evaporation dominant condition.

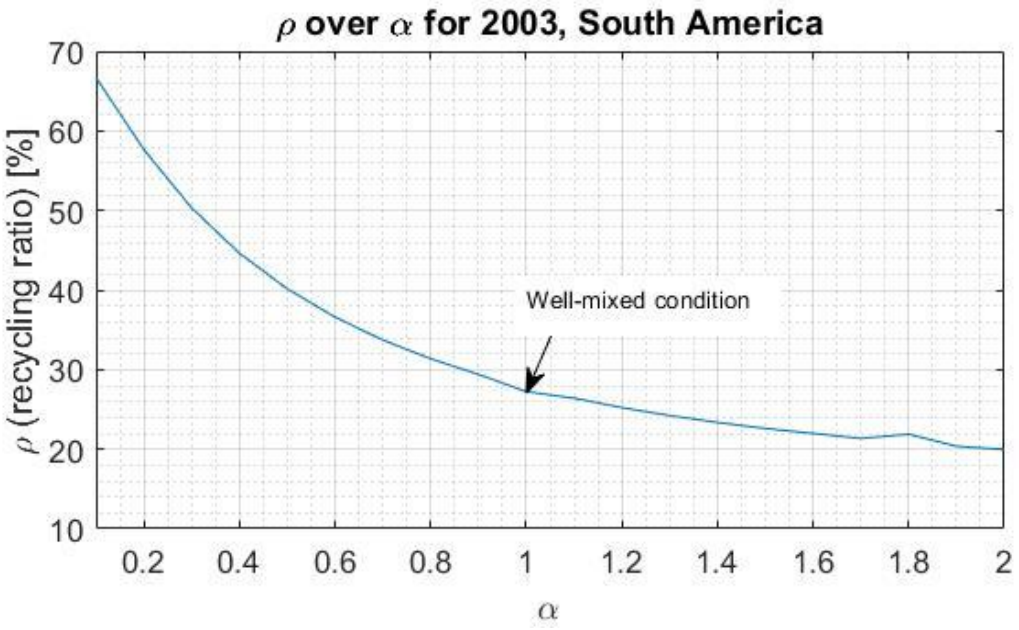

Figure 9 Computation of ρ with α range from 0.1 to 2.

The spatial distributions of annual mean ρ for 2003 with different α values are shown in Figures 10-12. The following figures contain annual mean recycling ratio for given α and annual mean water vapor fluxes in order to demonstrate the influence of wind velocities coupled with specific humidity on the spatial distributions of recycling ratio.

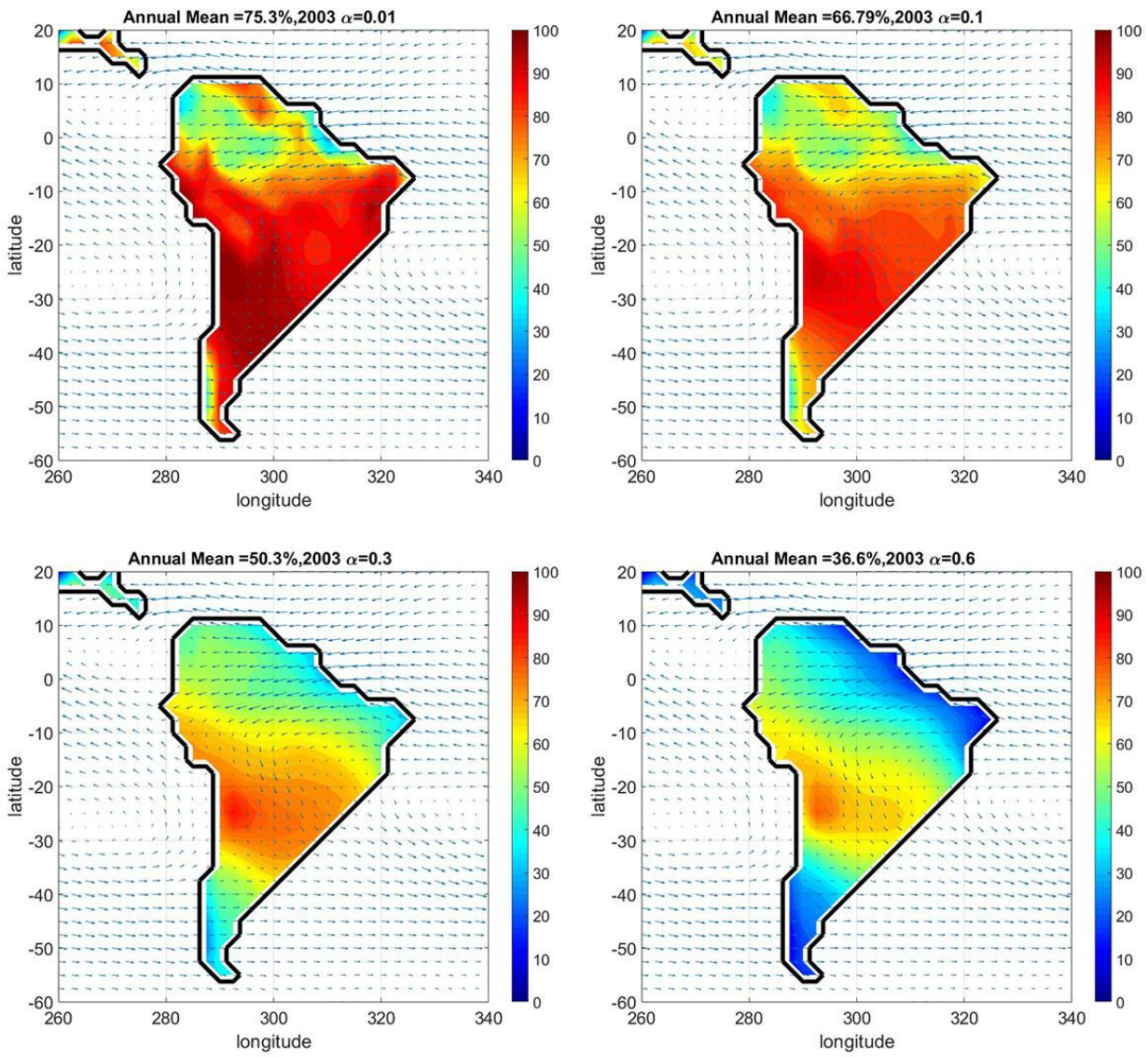

Figure 10 Distribution of ρ in South America for 2003, α as 0.01, 0.1, 0.3, 0.6. The arrow vectors indicate the directions and magnitudes of mean annual advection of water vapor.

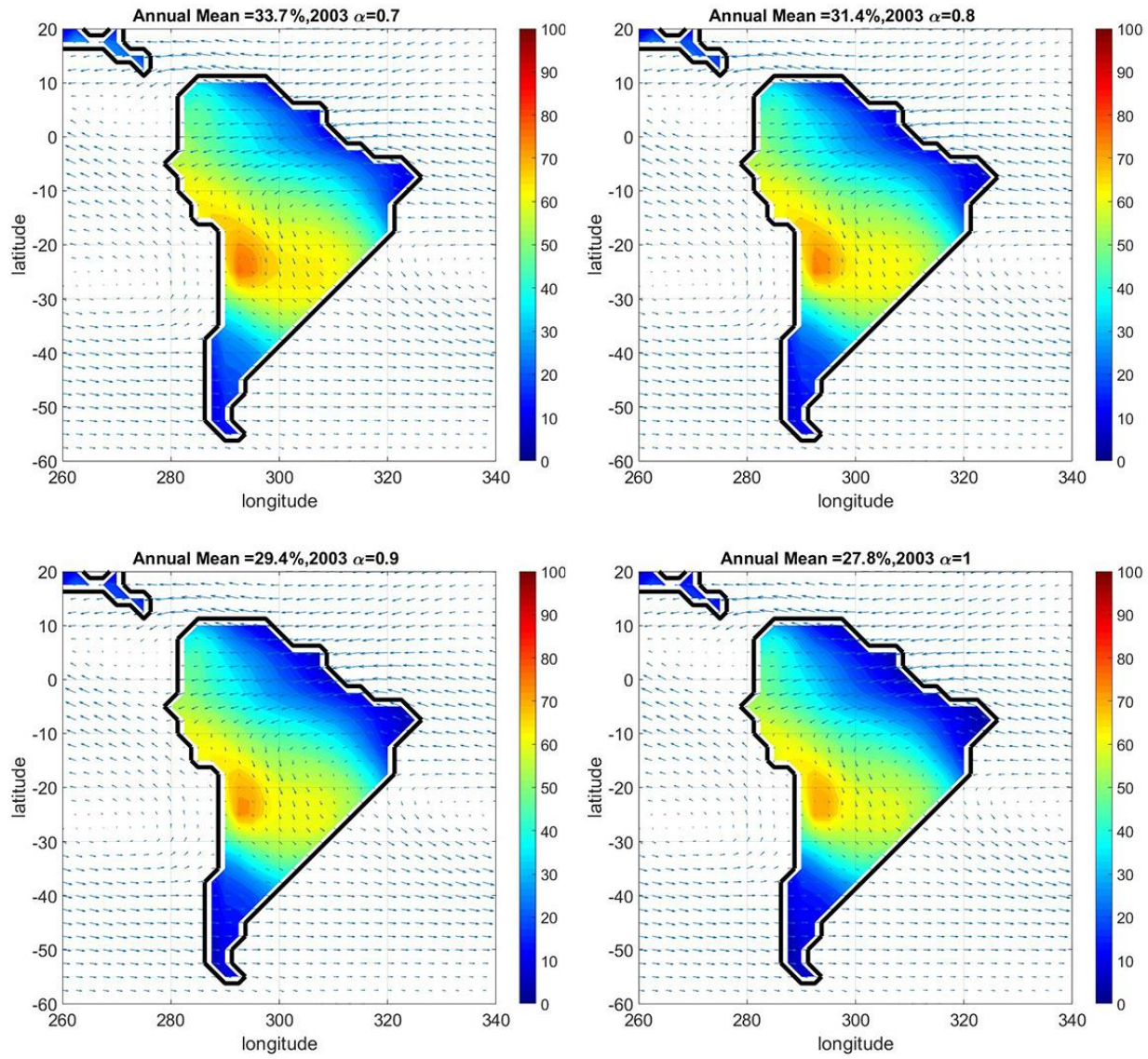

Figure 11. Distribution of ρ of South America for 2003 with α as 0.7, 0.8, 0.9, 1. The arrow vectors indicate the directions and magnitudes of mean annual advection of water vapors.

Figure 11 presents a distribution of recycling ratio over South America for 2003 for α as 0.7, 0.8, 0.9, and 1 (well-mixed condition)

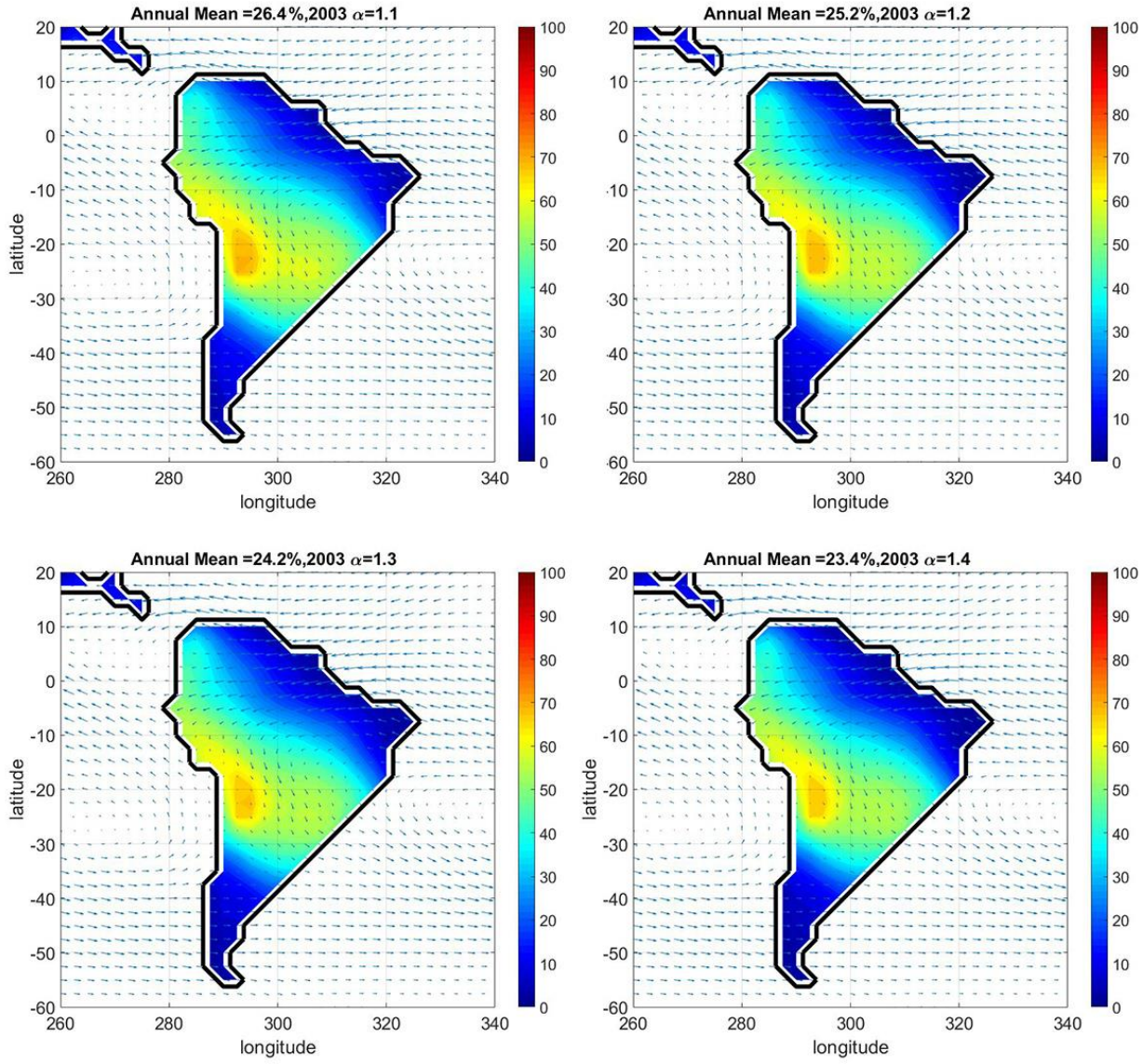

Figure 12. Distribution of ρ of South America for 2003 with α as 1.1, 1.2, 1.3, 1.4. The arrow vectors indicate the directions and magnitudes of mean annual advection of water vapor.

Figure 12 shows the distribution of ρ over South America for 2003 for α as 1.1, 1.2, 1.3, 1.4. α values for the above figures are selected so that they are close to well-mixed condition or α is equal to one.

The change of ρ for the area in the Atacama Desert of Peru around 20° S and 290° E is less influential by the change of α than other areas over the change of α and the corresponding

recycling ratio values are high with different α values. Over this area, advective water vapor is low as shown in Figure 10. The reason for the small advection is following. The on-shore wind from the Pacific Ocean is too cold to pick up enough moisture from the Pacific Ocean due to low temperature of Humboldt current (the Peru current), which is considered as one of the major reasons for the Atacama Desert hyperaridity (Sepulchre, Sloan et al. 2009). The west slope of the central Andes exhibits a rainfall shadow effect since the east side receives substantial rainfall resulting from advective water vapor from the Amazon basin. Limited supply of advective water vapors and the topographical blockage due to the Andes could be the reasons for high ρ in the Atacama Desert. In Figure 11 and 12, the Atacama Desert shows high value of precipitation recycling ratio. We conclude that topography and atmospheric circulations can strongly influence the spatial distribution of ρ. Another case of small change of α is shown in Figure 13 below.

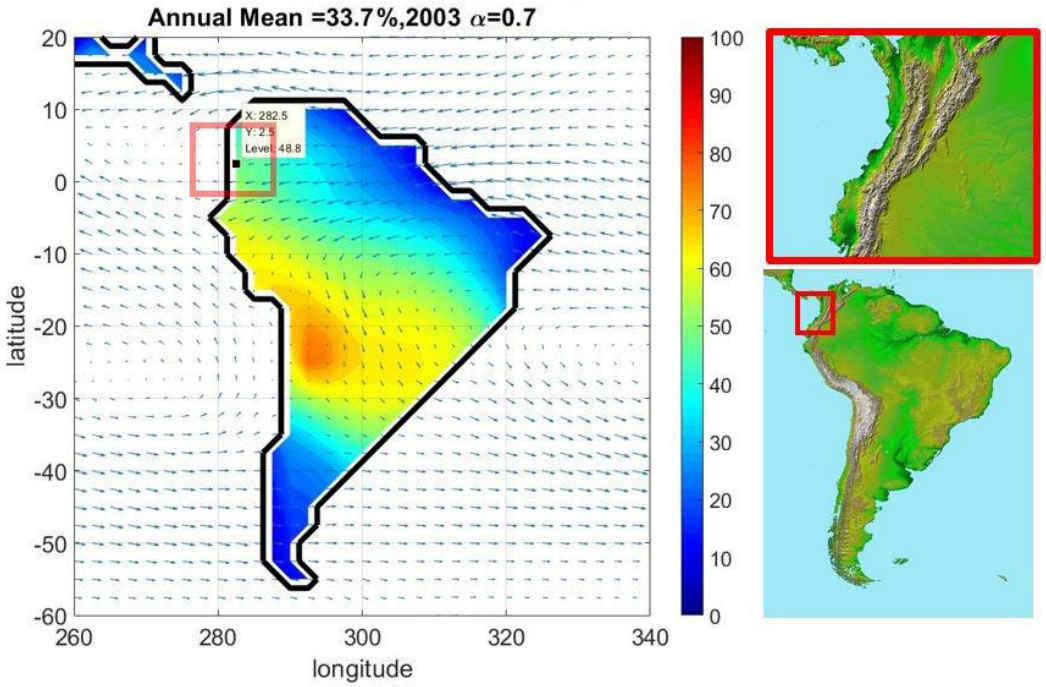

Figure 13. Distribution of ρ over South America, α as 0.7, South America continent. An area in the red box shows a possible place for rain shadow and its advection vector has relatively small size.

In Figure 13, the areas in the red box experiences small changes compared to other areas. It is Esmeraldas area of Ecuador. Its advection vector is relatively small. The advection vector at that point is -63.38 [kg/(m*yr)], 14.04 [kg/(m*yr)] as U, V vectors which positive direction of U vector is from West to East and positive direction of V vector is from South to North. P changes from 50.79% to 43.88% while α increases from 0.5 to 1.5. To compare the changes of ρ in that area with average change of ρ for South America at 2003, ρ for each case is plotted in Figure 14 below.

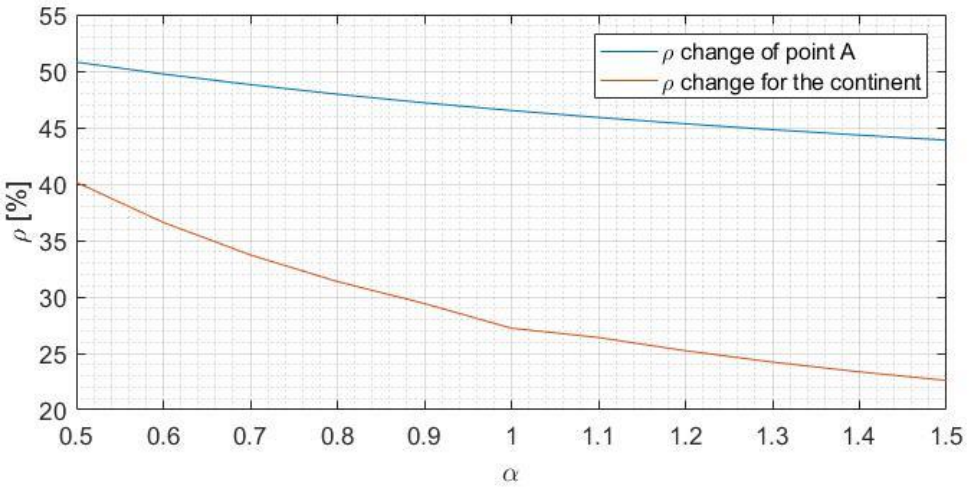

Figure 14.Comparison of change of ρ for the point A with those for the South America continent while α increases from 0.5 to 1.5. Change of ρ at point A is much smaller than those of the domain (South America)

Possible explanations of small change of ρ for the point A would be related with topological aspect of the area and size and direction of its advection vector. Again, the Andes would play a major role in the precipitation distribution and blocking moisture from the west of the Andes mountains.

The second charateristic is that the contribution of α to the recycling ratio is always negatice, but the sentivity of ρ to α becomes weaker as α increases. Another question is whether the charatersitics in 2003 is year specific. In the cahpter 4.3, a series of simulations will be conducted for the period from 1992 to 2006 in order to find the answer.

4.3 Simulations of recycling ratio ρ from 1992 to 2001 and 2004, 2006 and 2007

ρ for the period from 1992 to 2006 except 2002-2003 were obtained from the numerical solutions of equation (16) as shown in Table 2 and Figure 15.

Table 3. ρ for the given years with α as 0, 0.5,0.7,1,1.5,2

Year	1992	1993	1994	1995	1996	1997	1998	1999	2000	2001	2004	2005	2006
alpha	ρ	ρ	ρ	ρ	ρ	ρ	P	ρ	ρ	ρ	ρ	ρ	ρ
0	1	1	1	1	1	1	1	1	1	1	1	1	1
0.5	41.6	39.3	38.6	42.6	40.6	39.7	40.9	39.8	40.1	38.9	39.8	39.2	38.5
0.7	36.0	33.1	32.3	37.1	34.4	32.7	34.9	34.2	33.9	32.9	33.7	33.2	32.2
1	31.0	27.4	26.6	32.1	28.8	26.2	29.5	29.2	28.1	27.6	28.2	27.7	26.5
1.5	26.7	22.6	21.9	27.5	23.9	20.1	24.8	25.0	23.1	23.1	23.7	22.9	21.5
2	24.5	20.2	19.5	25.1	21.5	16.9	22.5	22.9	20.5	21.0	21.4	20.5	19.0
5	20.4	15.8	14.9	20.6	16.9	10.8	18.1	18.7	15.3	17.1	17.5	15.8	14.0
15	17.7	13.0	12.0	17.9	14.1	8.0	15.2	15.9	11.7	14.7	15.1	12.9	10.7

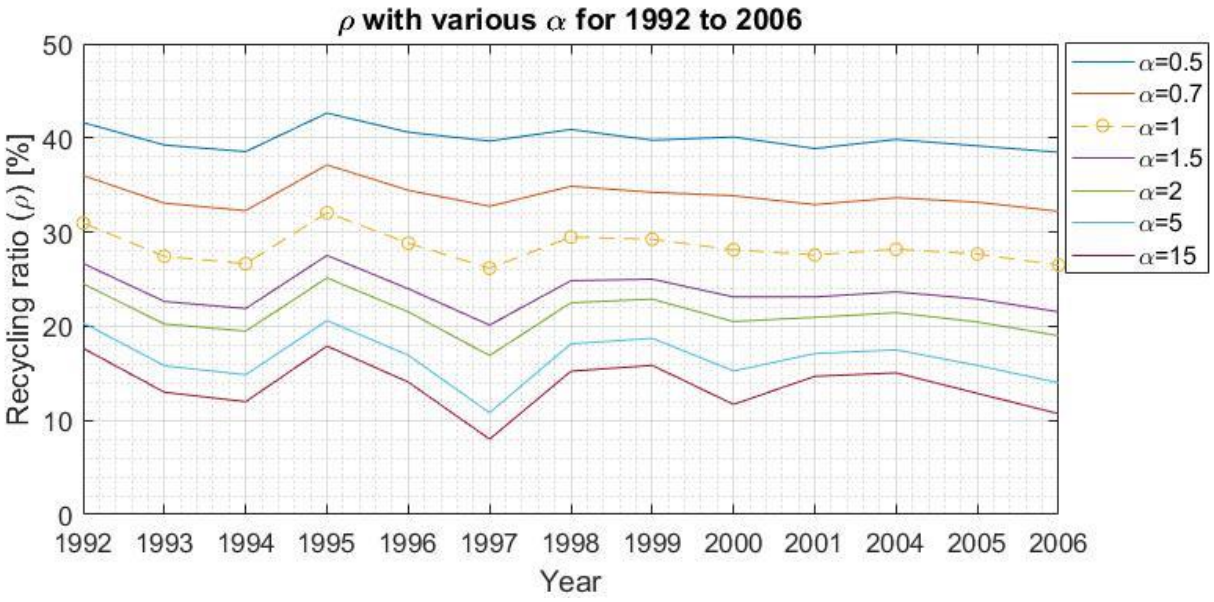

Figure 15. ρ from 1992 to 2006 except 2002,2003 with various α. α values are 0.5, 0.7, 1, 1.5, 2, 5, 15.

A shown in Figure 15, as α gets greater, ρ becomes smaller. It is evident that the pattern of α for 2003 prevails throughout the study period.

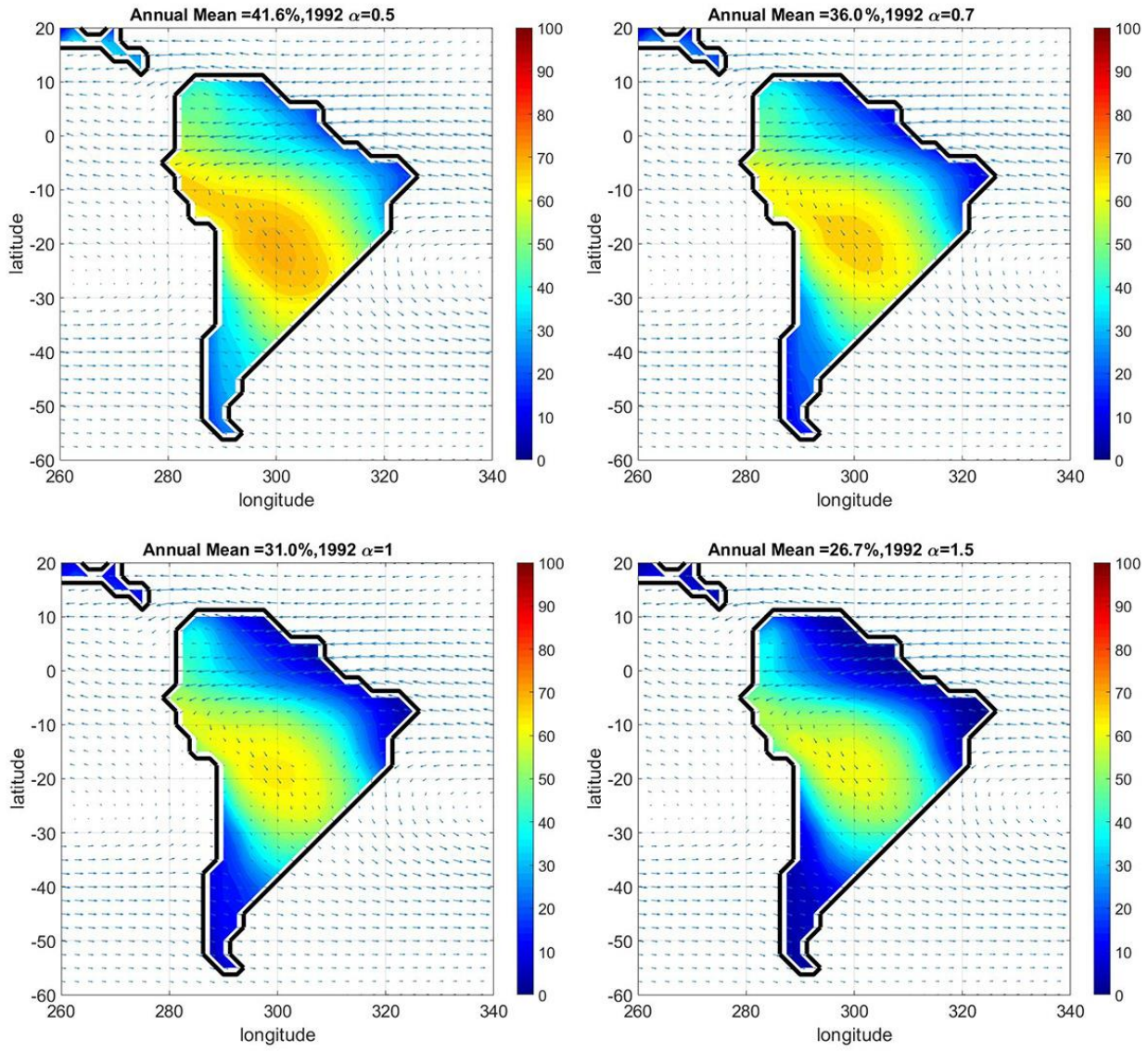

Figure 16. ρ distribution for 1992 α as 0.5, 0.7, 1, 1.5. It shows a negative contribution of α to ρ. The arrow vectors indicate the directions and magnitudes of mean annual advection of water vapor.

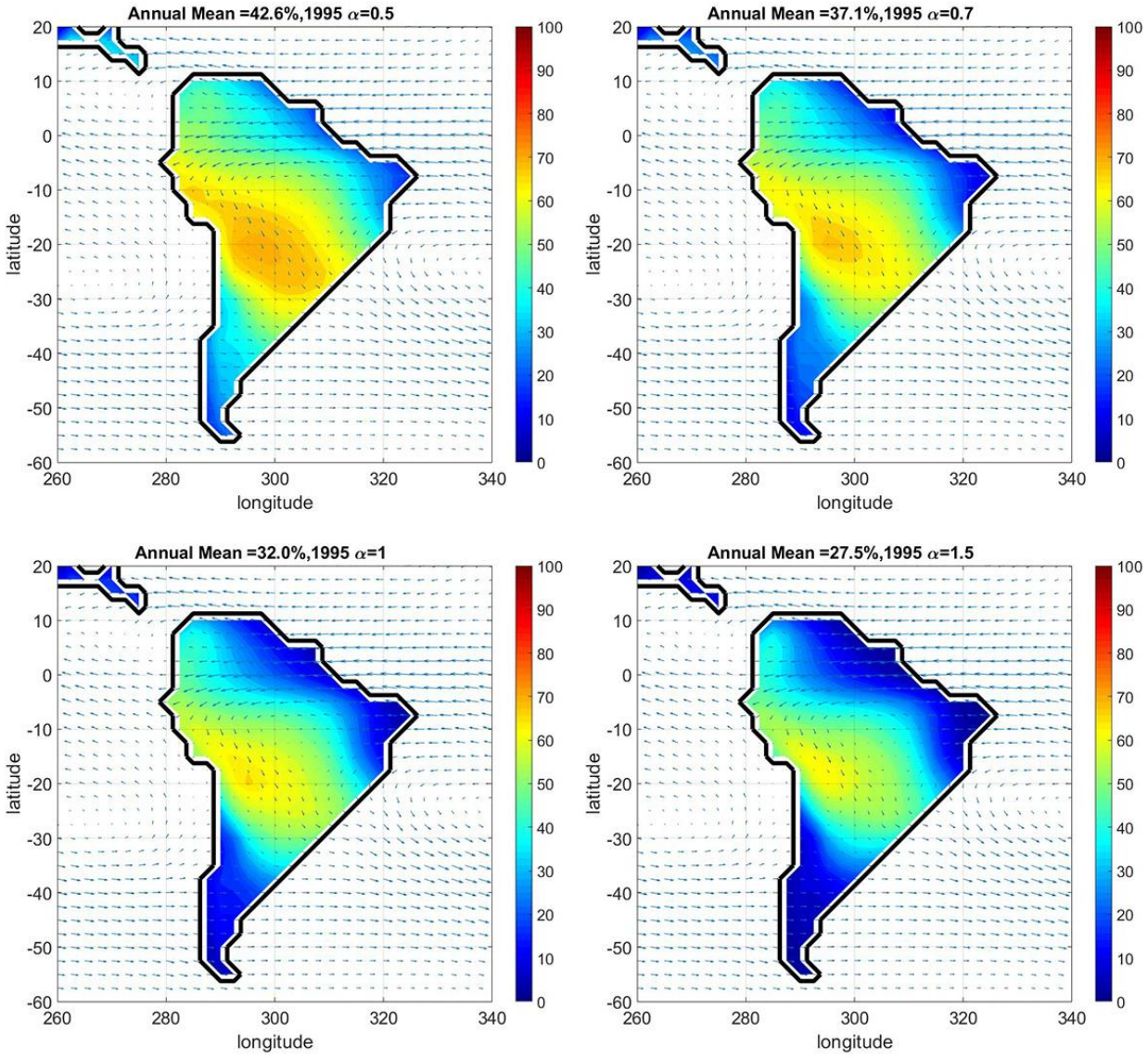

Figure 17. ρ distribution for 1995, α as 0.5, 0.7, 1, 1.5. It shows a negative contribution of α to ρ. The arrow vectors indicate the directions and magnitudes of mean annual advection of water vapor.

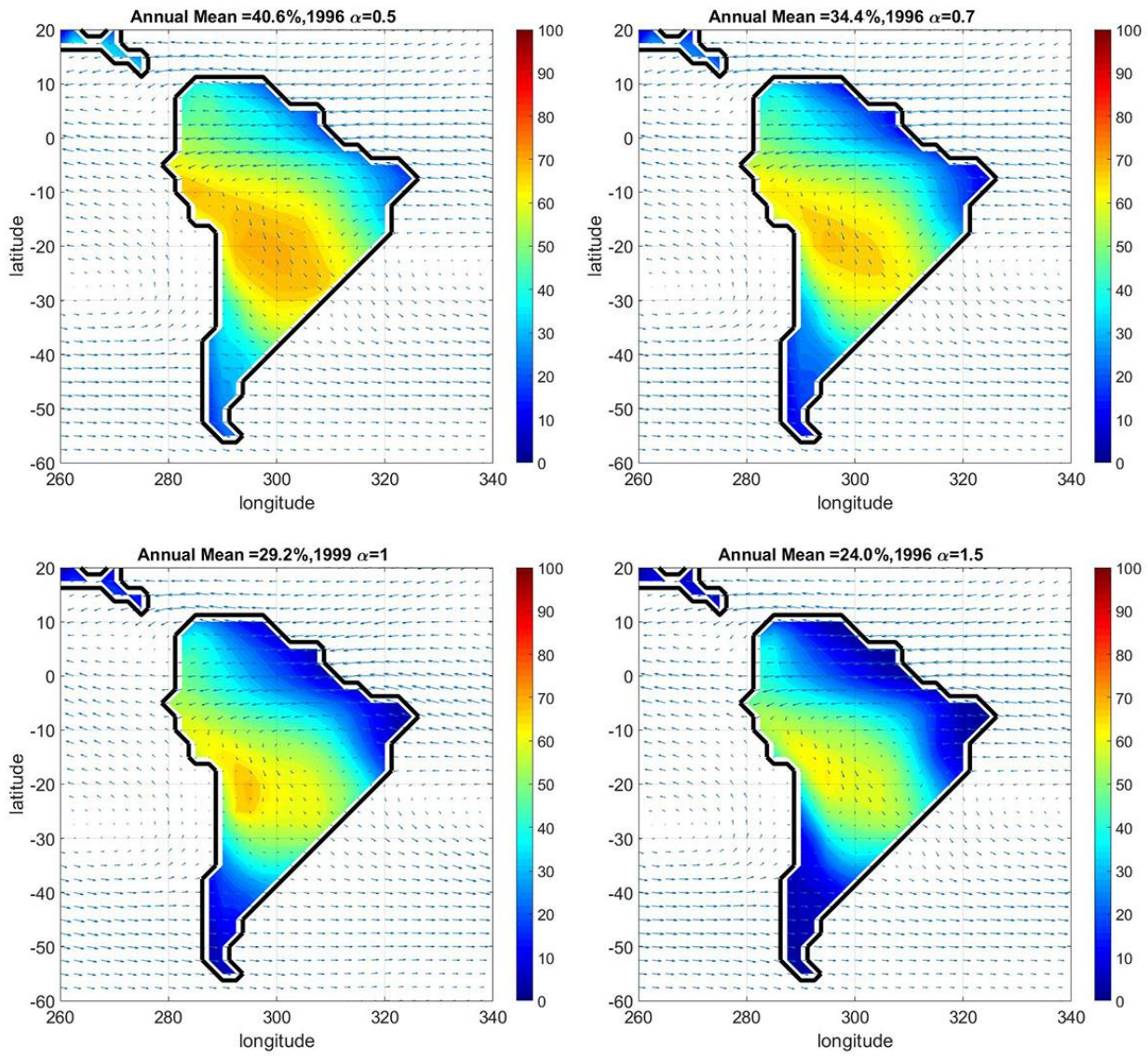

Figure 18. ρ distribution for 1996, α as 0.5, 0.7, 1, 1.5. It shows a negative contribution of α to ρ. The arrow vectors indicate the directions and magnitudes of mean annual advection of water vapor.

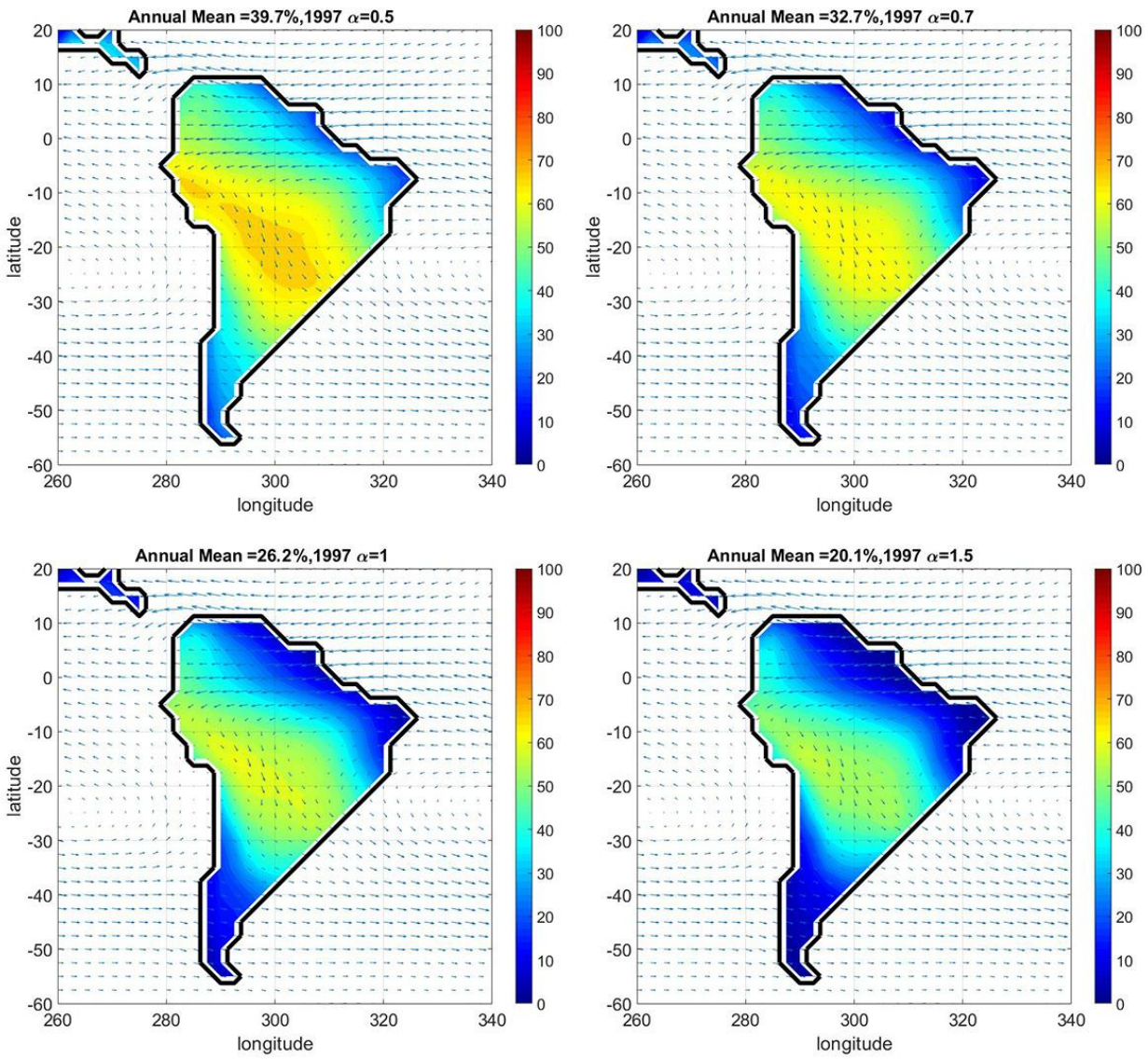

Figure 19 ρ distribution for 1997, α as 0.5, 0.7, 1, 1.5. It shows a negative contribution of α to ρ. Th arrow e vectors indicate the directions and magnitudes of mean annual advection of water vapor.

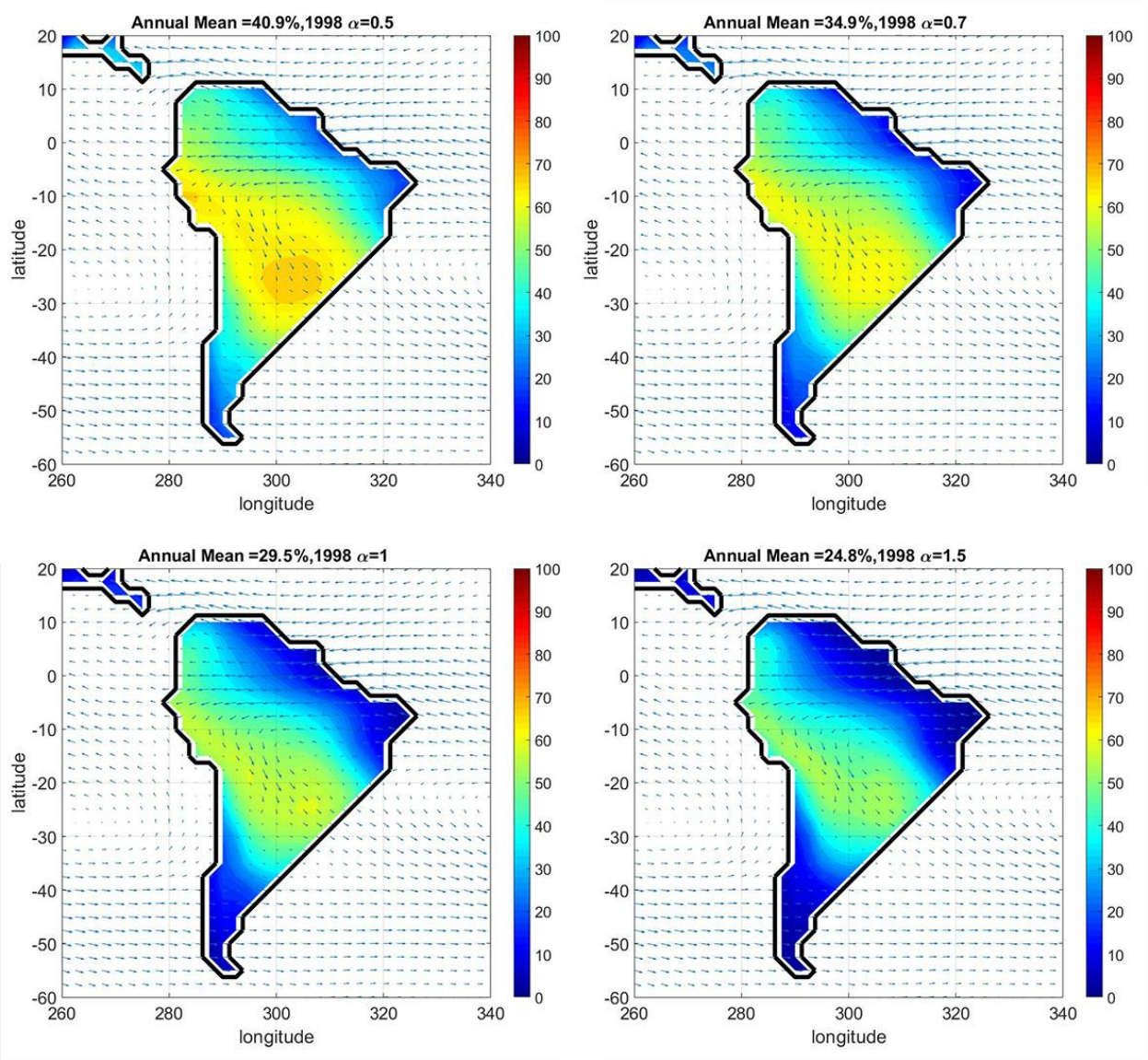

Figure 20 ρ distribution for 1998, α as 0.5, 0.7, 1, 1.5. It shows a negative contribution of α to ρ. The arrow vectors indicate the directions and magnitudes of mean annual advection of water vapor.

As shown in Figures 16, 17, 18, the overall distributions of ρ are similar. Yet, as shown in Figures 16-18, the maximum ρ are located around the Pacific Ocean, which is different from those of Figures 19-20. An exception is 1998, the locations for the maximum of ρ are around 25° S and 306° E and 10° S and 285° E close to the Atlantic Ocean. During 1997~1998, the El Nino was the strongest and the extreme weather events occurred globally. El Nino influences the

South America in many ways such as heavy precipitation in the southern Brazil. During EN (El nino), the enhanced weakening of the subtropical jet in spring with advection of cyclonic (anticyclonic) vorticity over southern Brazil, and of the deepening west low strengthened northerly advection of moisture (Grimm, Barros et al. 2000). If the advection brought more moisture to the southern Brazil, the location of the maximum ρ would be pushed eastward due to the strong moisture advection. The moving direction of the maximum ρ of 1997 and 1998 from maximum locations for other years is very similar to the direction of water vapor flux. This phenomenon could explain the shift of the location of maximum ρ. And the precipitation characteristic in 1997-1998 might explain low values of ρ compared to other years. The precipitation of the South American continent during strong El Nino period is incurred by strong advection, implying that ρ decreases with precipitation incurred by strong advection. That hypothesis is more likely to hold with the definition of precipitation recycling ratio. For these reasons, El Nino is another strong factor to determine magnitude and distribution of ρ. Further research would consider the effect of El Nino and Southern Oscillation (ENSO) on the distribution of ρ.

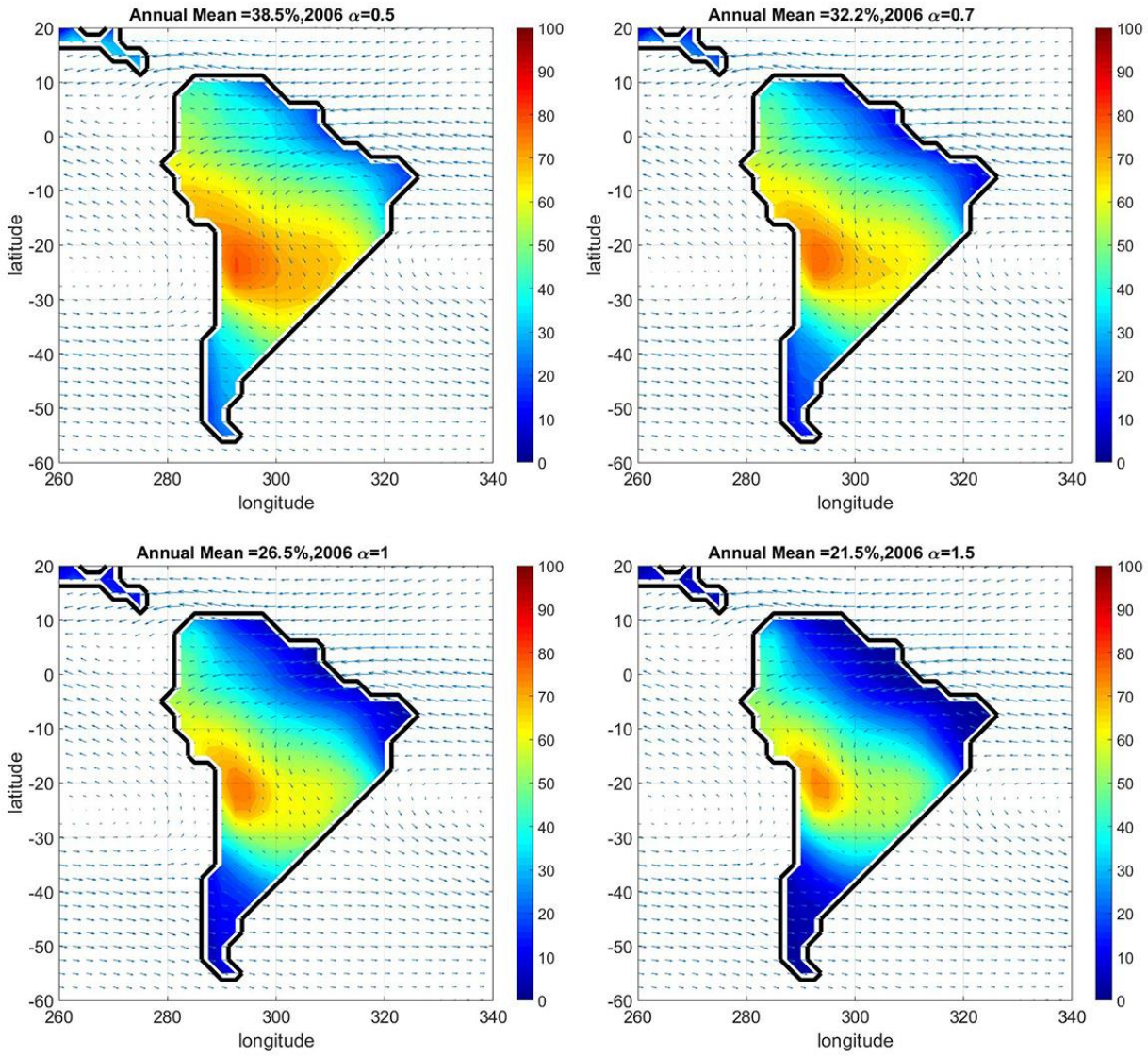

Figure 21 ρ distribution for 2006, α as 0.5, 0.7, 1, 1.5. The arrow vectors indicate the directions and magnitudes of mean annual advection of water vapor.

Influence of topography and advection vector is evident as shown in the above figures. The Andes appears to be a barrier separating the Atacama Desert from the Amazon basin. The mountainous regions have higher ρ, especially over the west side of the Andes. Foley et al (2005) studied the role of the Andes mountains in precipitation over the South America, especially the Amazon basin and Desert Atacama. The Andes acts as a barrier separating arid region to the west in the Peru-Bolivian Atacama Desert from wet regions to the east in the

Amazon Basin and the Andes mountains that blocks tropospheric flow resulting in a rain shadow over the Altiplano. In addition, water vapor flux plays an important role in the distribution of ρ as mentioned previously in 4.2. It shows that the location of maximum ρ might move along water vapor flux

4.4. Contribution of Precipitation and Evaporation to modeling ρ

Evaporation and precipitation are major input variables of the governing equation for ρ. A series of simulations were performed to understand the effects of evaporation and precipitation on ρ under not well-mixed conditions. As input variables of the simulations, arbitrary matrices (netcdf file) of precipitation and evaporation were made. The spatial and temporal resolution of the input data sets are 2.5 °×2.5° and 6 hourly. The matrix size is 192x94x1460 (longitude x latitude x time) for each year. First, annual mean values for all grid points in the South America for 2007 were calculated. Evenly distributed sixteen values from zero to maximum annual mean precipitation rate were selected shown in Table 4. A list for evaporation rate is also shown in Table 4.

Table 4 Evaporation rates and precipitation rate for simulation for 4.4

P [mm/day]	P [mm/day]	E [mm/day]	E [mm/day]
0	5.33	0	1.71
0.2	6.06	0.13	1.93
0.93	6.79	0.36	2.16
1.66	7.53	0.58	2.38
2.4	8.26	0.81	2.61
3.13	9.00	1.03	2.83
3.86	9.73	1.26	3.06
4.59	10.46	1.48	3.28

For example, one matrix has identical elements being 5.33 [mm/day] or 0.0000701 [kg/m^2/s] as the unit of the input data file. 16 arbitrary matrices are made for precipitation and another 16 matrices for evaporation. Total 64 simulations were conducted with 32 matrices for each not well-mixed condition, 32 simulations were performed under the LED condition and 32 simulations under the AD condition. For simulations on the contribution of precipitation to ρ, the data set of evaporation is the same as the original evaporation data of 2007. For simulations on the contribution of evaporation to ρ, precipitation data set is the original data set of 2007. The simulations for the contribution of precipitation to ρ under LED condition is presented in Table 5. The simulations for the contribution of evaporation to ρ under LED condition is presented in Table 6. Table 7 shows the simulations on the contribution of P to ρ under the AD condition. Table 8 shows the simulations on the contribution of E to ρ under AD condition.

4.4.1 ρ under LED condition

Table 5 Change of ρ over different precipitation rates for 2007, α is 0.7

P [mm/day]	0	0.20	0.93	1.66	2.40	3.13	3.86	4.59
rho [%]	38.3	38.2	37.7	37.1	36.5	35.9	35.3	34.7
P [mm/day]	5.33	6.06	6.79	7.53	8.26	9.00	9.73	10.46
rho [%]	34.1	33.5	32.8	32.1	31.4	30.8	30.1	29.4

Distribution of ρ with a new list of matrix for P are plotted below as Figure 22, 23.

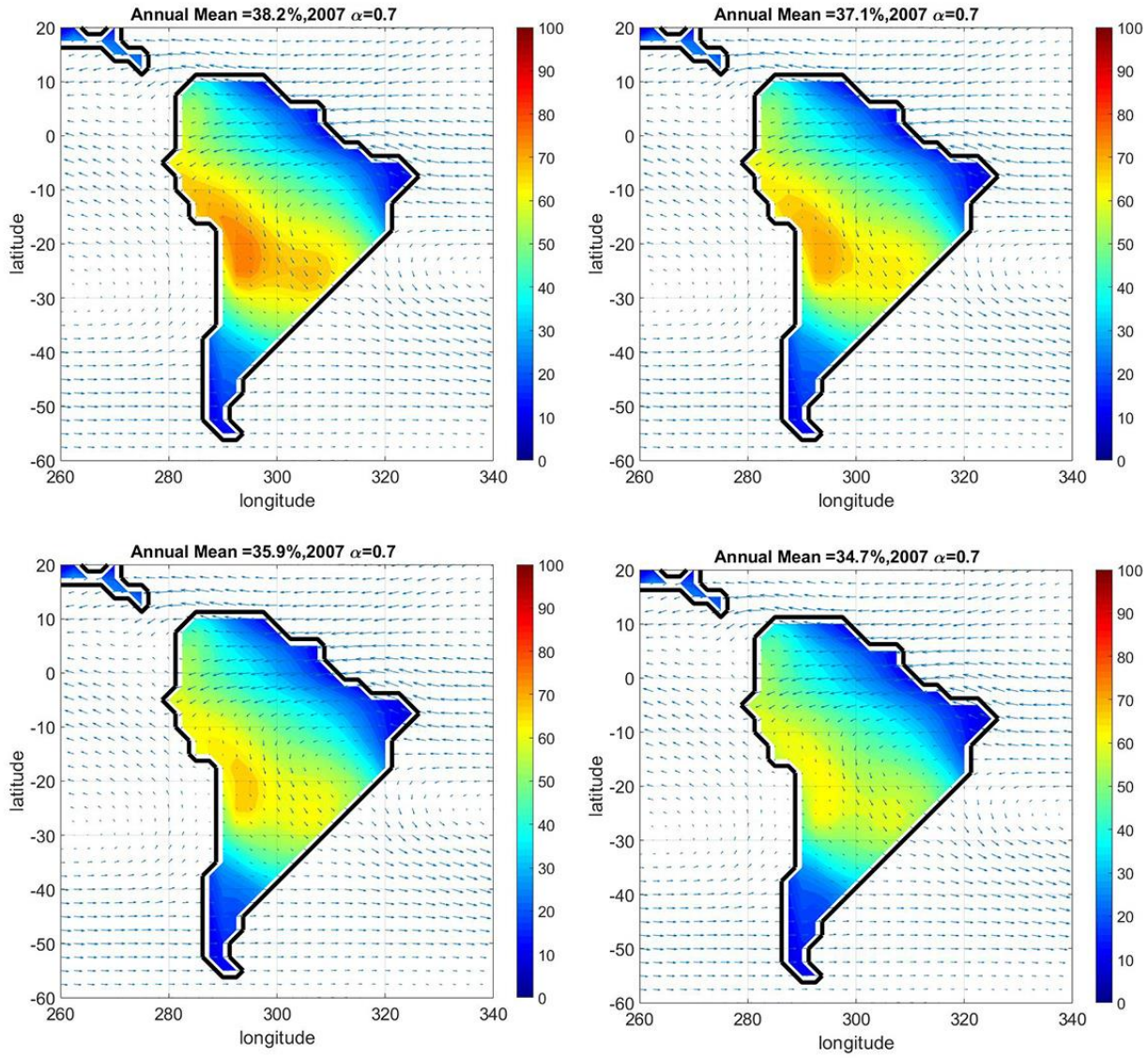

Figure 22 ρ distribution for 2007 with different precipitation amount, α as 0.7. The applied P amounts are 0.197, 1.66, 3.13, 4.60 [mm/day] from top left in clock wise direction. The figure show negative contribution of P to ρ. The vectors arrow indicates the directions and magnitudes of mean annual advection of water vapor.

In Figure 22, P has a negative contribution under LED condition. P used in the ρ model shown in the following panels are 6.06, 7.53, 8.99, 10.46 [mm/day], respectively, from left top to left bottom clockwise.

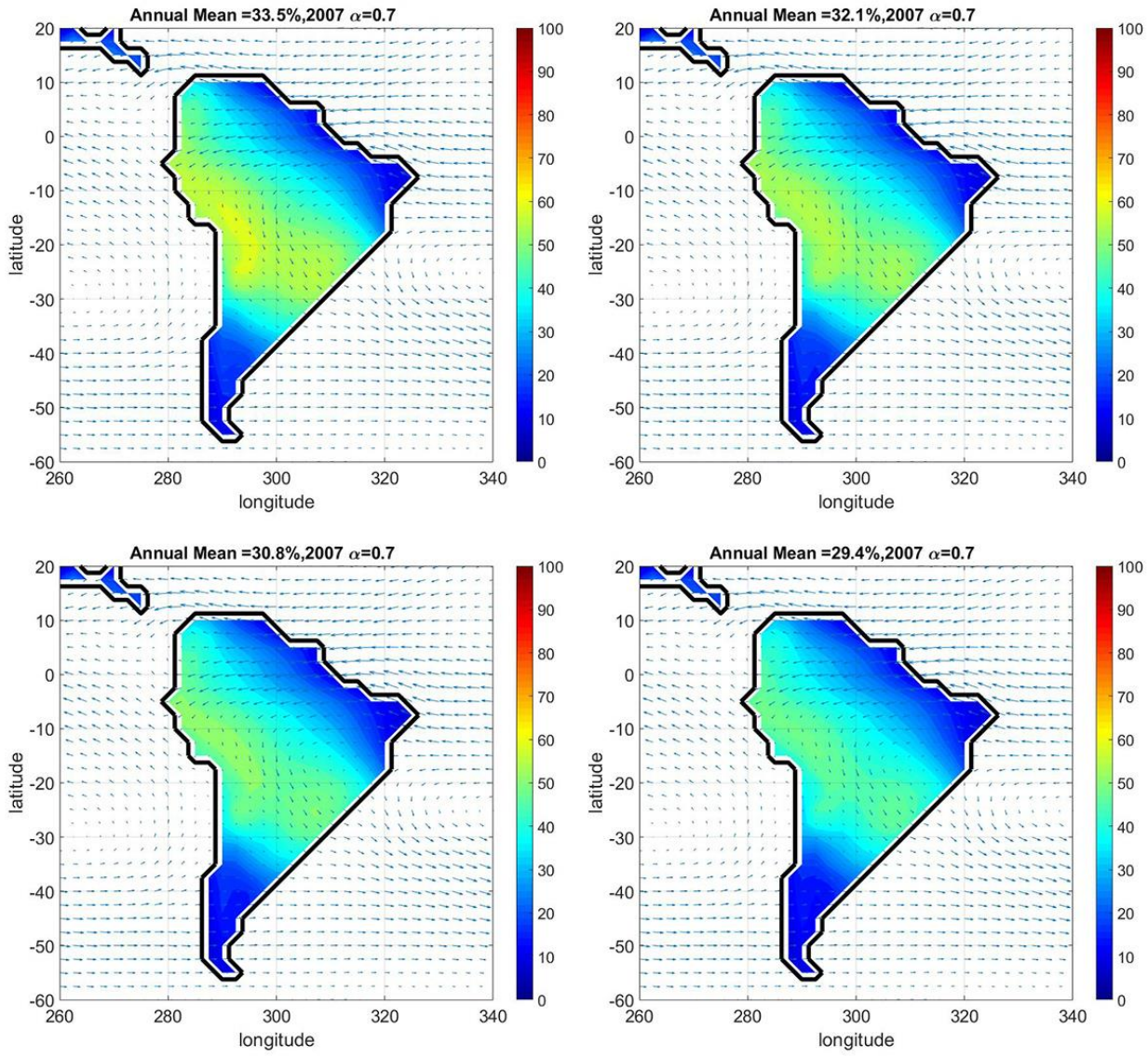

Figure 23 ρ distribution for 2007 with different precipitation amount, α as 0.7. The applied P amounts are 6.06, 7.53, 8.99, 10.46 [mm/day] from top left in clock wise direction. The figure show negative contribution of P to ρ. The vectors indicate the directions and magnitudes of mean annual advection of water vapor.

Figures 22-23 show that precipitation has negative contribution to ρ.

Table 6. change of ρ over different Evaporation rates for 2007, α as 0.7

E [mm/day]	0	0.13	0.36	0.58	0.81	1.03	1.26	1.48
rho [%]	0	2.7	6.2	9.2	11.9	14.4	16.8	18.9
E [mm/day]	1.71	1.93	2.16	2.38	2.61	2.83	3.06	3.28
rho [%]	20.9	22.8	24.6	26.2	27.8	29.3	30.7	32.0

Annual mean evaporation rates corresponding to the following Figure 24 are 0.132, 0.583, 1.03, 1.48 [mm/day] clockwise from top left to bottom left. In Figure 25, evaporation rates corresponding to each panel are 1.93, 2.38, 2.83, 3.28 [mm/day], respectively from top left to bottom left in clock wise direction.

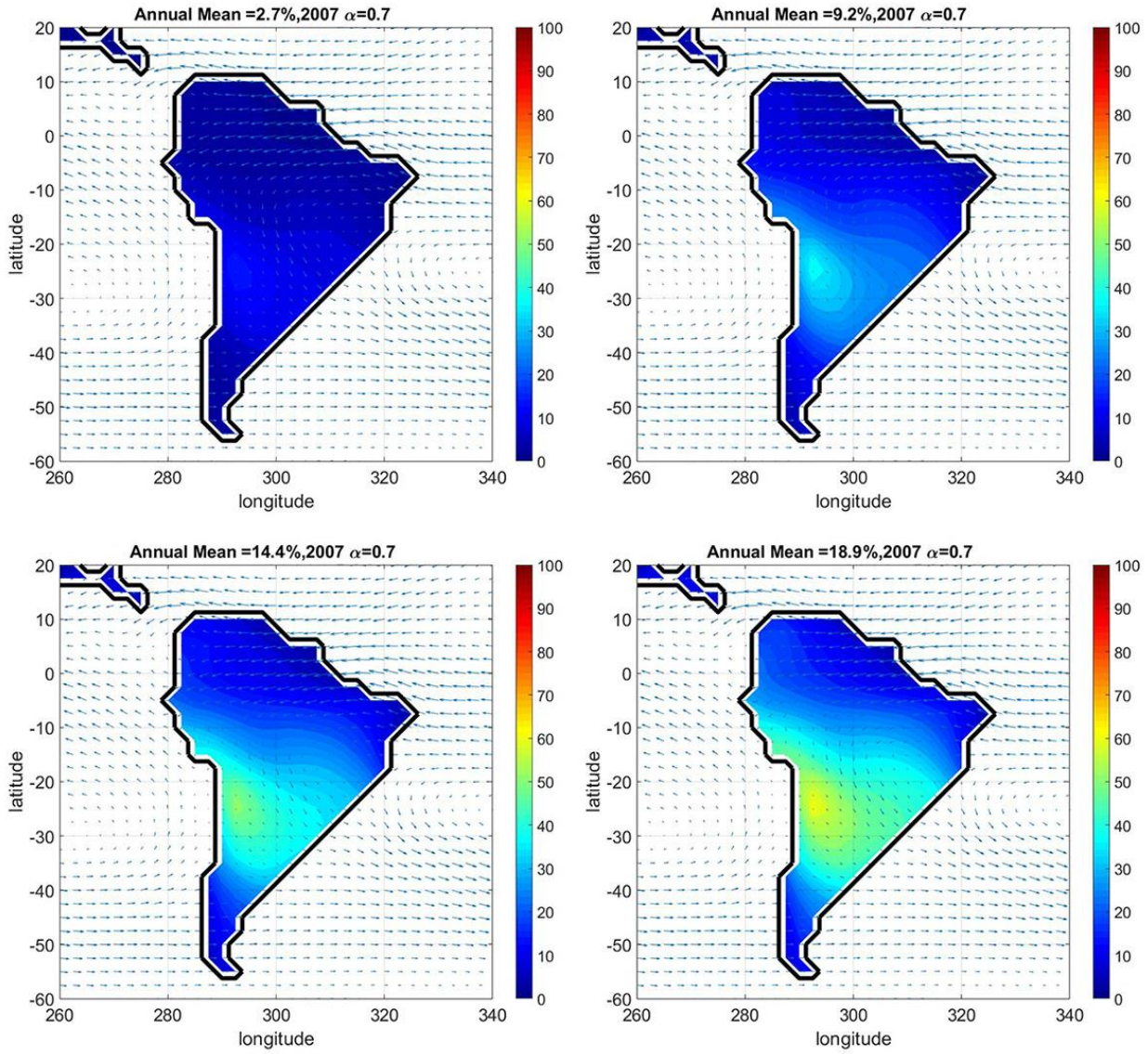

Figure 24 ρ distribution for 2007 with different evaporation rates, α as 0.7. The applied E rates are 0.13, 0.58, 1.03, 1.48 [mm/day] from top left to bottom left images in clock wise direction. It shows that E has positive contribution to ρ. The vectors indicate the directions and magnitudes of mean annual advection of water vapor.

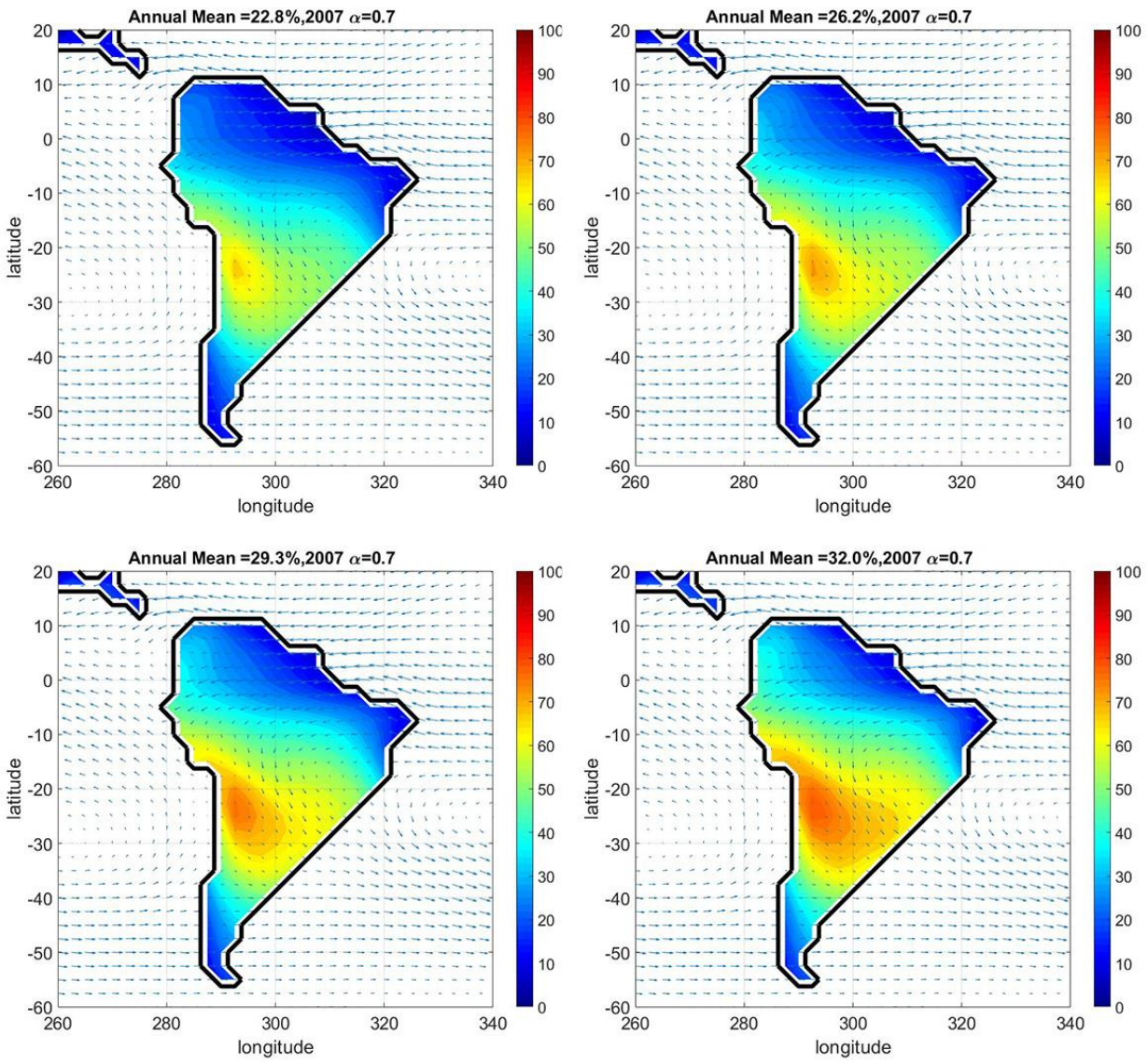

Figure 25 ρ distribution for 2007 with different evaporation rates, α as 0.7. The applied E rates are 0.13, 0.58, 1.03, 1.48 [mm/day] from top left to bottom left images in clock wise direction. It shows that E has positive contribution to ρ. The vectors indicate the directions and magnitudes of mean annual advection of water vapor.

As shown in the above figures, evaporation has positive contribution to ρ under LED condition. Therefore, evaporation and precipitation have conditional contribution to the precipitation recycling ratio depending on the types of not well-mixed condition. According to equation (16)

$$\frac{\partial \rho}{\partial t} + \frac{\overrightarrow{F_q}}{w} \cdot \nabla \rho = \alpha \left(\rho^{1-\frac{1}{\alpha}} - \rho \right) \frac{E}{w} \; - \alpha \left(\rho^{2-\frac{1}{\alpha}} - \rho \right) \frac{P}{w}$$

the first term on the right-hand side (RHS) of the equation is always positive under local evaporation dominant t condition. But the second term with negative sign, $-\alpha \left(\rho^{2-\frac{1}{\alpha}} - \rho \right) \frac{P}{w}$ is always negative under the LED condition. If an area under LED condition, increased precipitation would contribute to recycling ratio in a negative way. Evaporation has positive contribution to the recycling ratio (ρ) under the LED condition. An interesting case is the site with low recycling ratio and strong advection from the oceans. An example for that is the area around 5° S, 320° E where ρ changes from 14.6 % to 11.6 % while P changes from 0.198 mm/day to 10.46 mm/day. At the same time, the mean ρ of the domain changes from 38.2 % to 29.4 % with the same changes of P. The magnitude and direction of advective water vapors are Uq=-274.4 [kg/ (m*yr)] Vq=79 [kg/(m*yr)], indicating that large amount of advective water vapors was transported from the Atlantic to the continent. Similar cases are found at 52.5° S, 287.5° E where strong advection of water vapors is found as U=192.3 [kg/(m*yr)], V=1.771 [kg/m*yr] with small change of ρ over P.

4.4.2 Computation of ρ under AD (advection dominant) condition

For computation of ρ under AD condition, 16 matrices are made for evaluating the effect of P on ρ while maintaining the other input variables unchanged. Another 16 matrices are for evaluating the effect of E on ρ while maintaining the other input variables the same as original values of 2007. The simulations for the impact of P on ρ are presented in Figures 26 and 27 while those of the impact of E on ρ are presented in Figures 28 and 29.

Table 7 Changes of ρ with different precipitation rates for 2007, α as 1.3

P [mm/day]	0	0.20	0.93	1.67	2.40	3.13	3.86	4.60
rho [%]	23.1	23.2	23.7	24.1	24.5	24.9	25.3	25.7
P [mm/day]	5.33	6.06	6.79	7.53	8.26	8.99	9.73	10.46
rho [%]	26.1	26.4	26.8	27.2	27.5	27.9	28.3	28.6

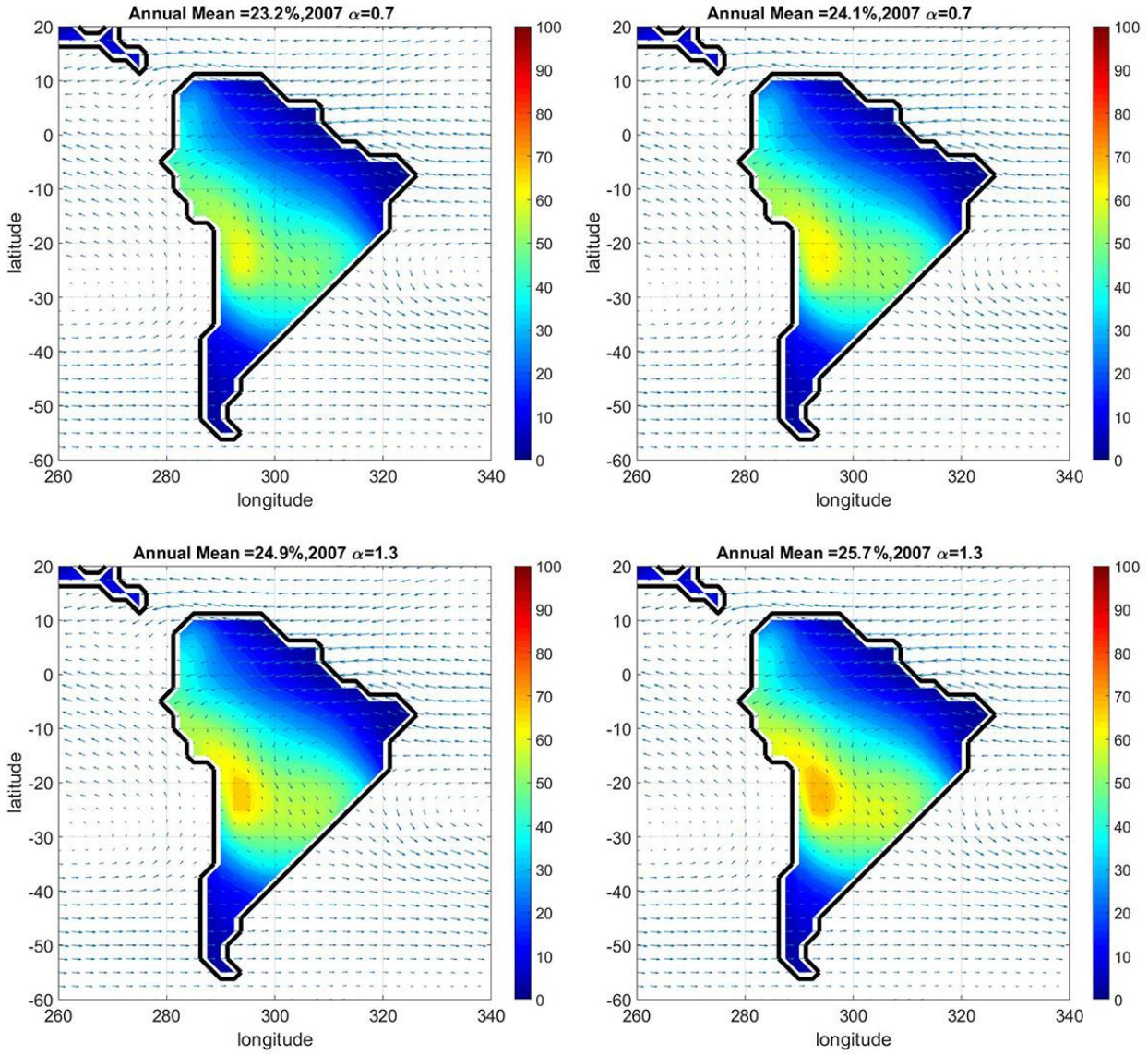

Figure 26. ρ distribution for 2007 with different precipitation rates, α as 1.3. The applied P rates are 0.20, 1.67, 3.13, 4.60 [mm/day] from top left to bottom left images in clock wise direction. It shows that P has positive contribution to ρ. The arrow vectors indicate the size and magnitude for advection of water vapors

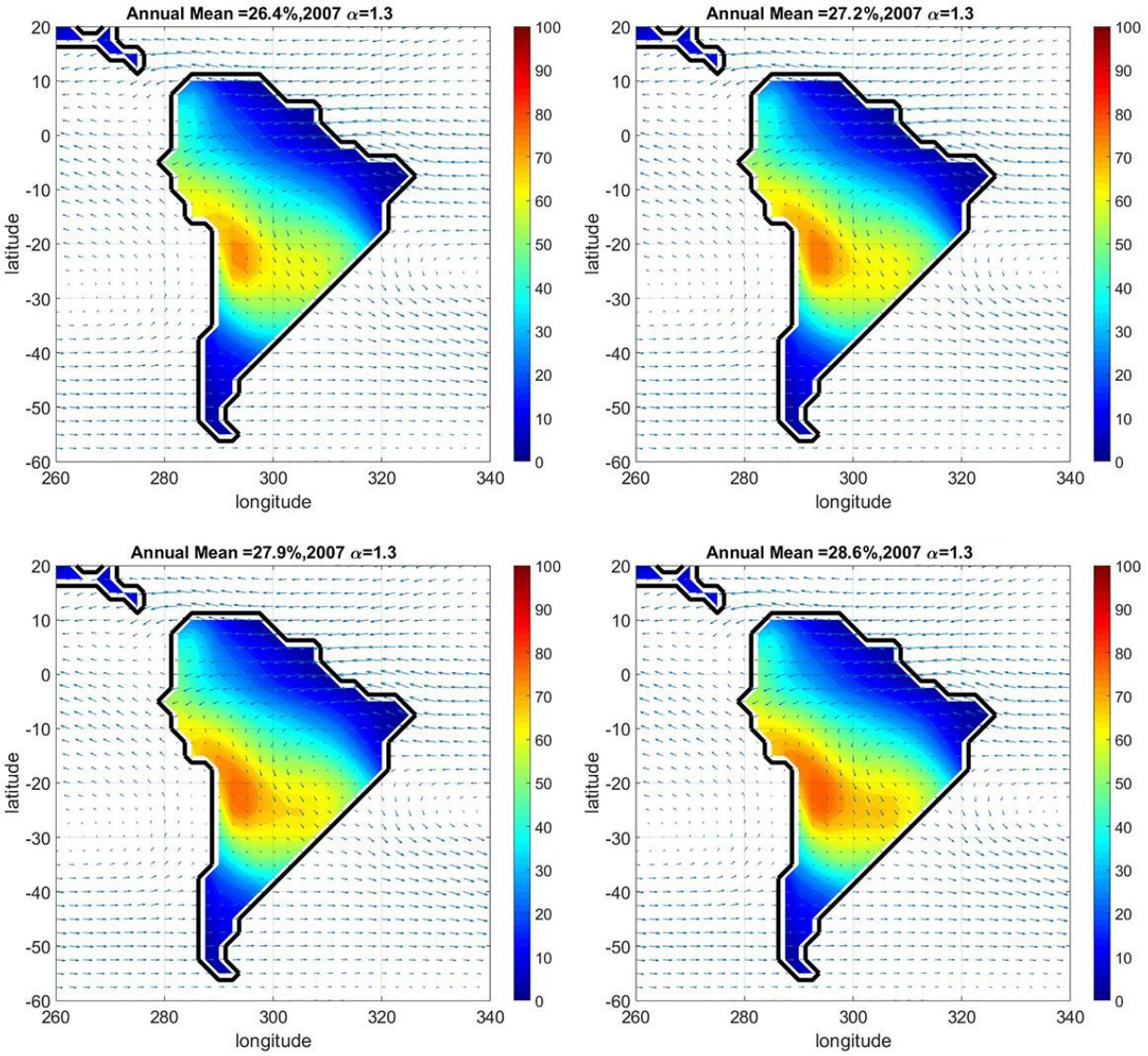

Figure 27 ρ distribution for 2007 with different precipitation amount, α as 1.3. The applied P rates are 6.06, 7.53, 8.99, 10.46 [mm/day] from top left to bottom left images in clock wise direction. It shows that P has positive contribution to ρ. The arrow vectors indicate the size and magnitude for advection of water vapors

Table 8. change of ρ with different evaporation rates, α as 1.3

E [mm/day]	0	0.13	0.36	0.58	0.81	1.03	1.26	1.48
rho [%]	0	1.9	4.6	6.9	9.0	10.9	12.6	14.2
E [mm/day]	1.71	1.93	2.16	2.38	2.61	2.83	3.06	3.28
rho [%]	15.8	17.1	18.5	19.7	20.9	22.0	23.1	24.1

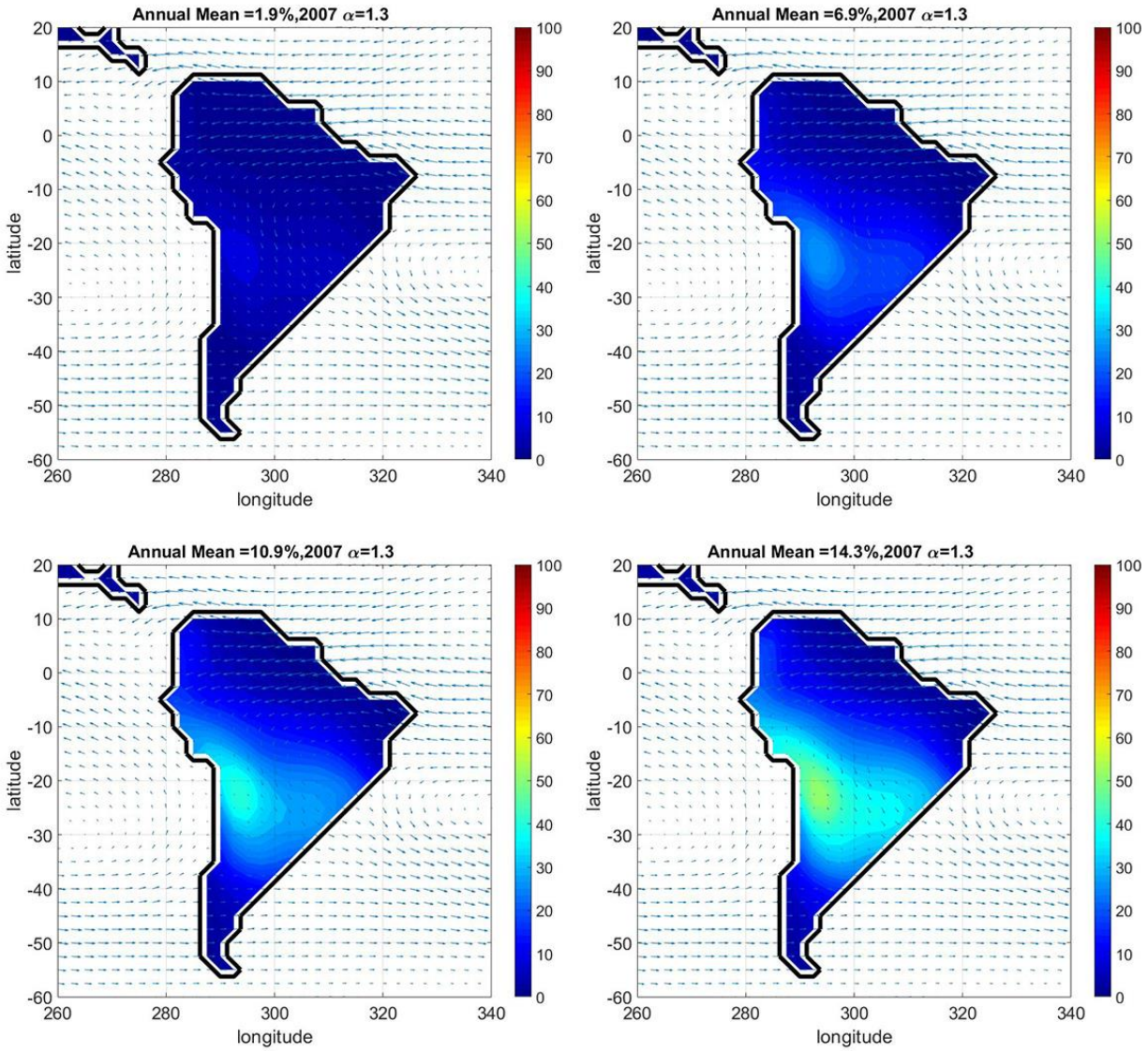

Figure 28 ρ distribution for 2007 with different evaporation rates, α as 1.3. The applied E rates are 0.13, 0.58, 1.03, 1.48 [mm/day] from top left to bottom left images in clock wise direction. The E has positive contribution to ρ. The arrow vectors indicate the size and magnitude for advection of water vapors

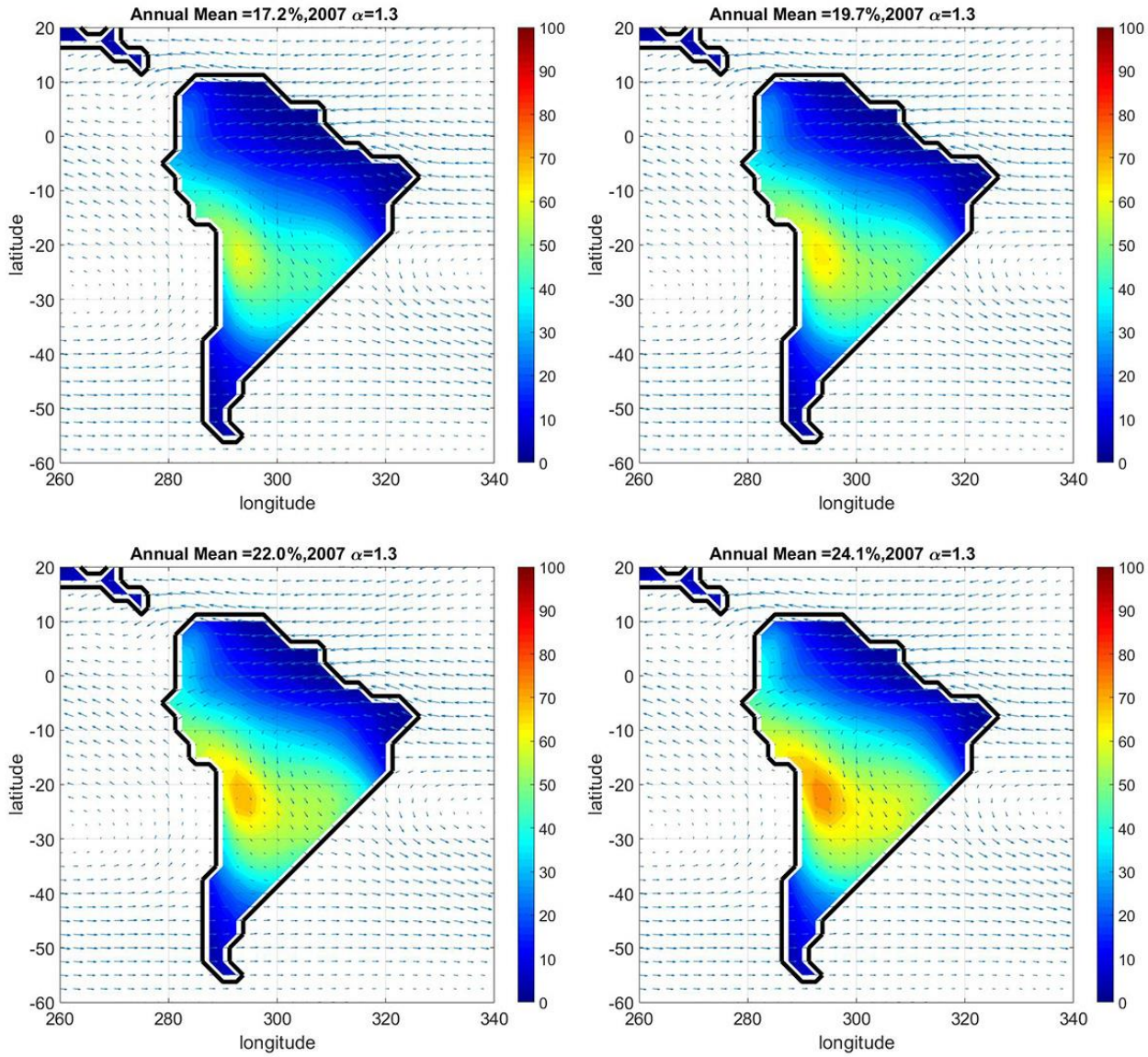

Figure 29 ρ distribution for 2007 with different evaporation rates, α as 1.3. The applied E rates are 1.93, 2.38, 2.83, 3.28 [mm/day] from top left to bottom left images in clock wise direction. The E has positive contribution to ρ. The arrow vectors indicate the size and magnitude for advection of water vapors

Figures 26-27 show positive contribution of precipitation to the recycling ratio. Since additional evaporation increases ρ according to equation (16), evaporation always has positive contribution to the recycling ratio under both (LED and AD) conditions. Figure 31 below demonstrates the contributions of E and P to the recycle ratio under LED and AD condition.

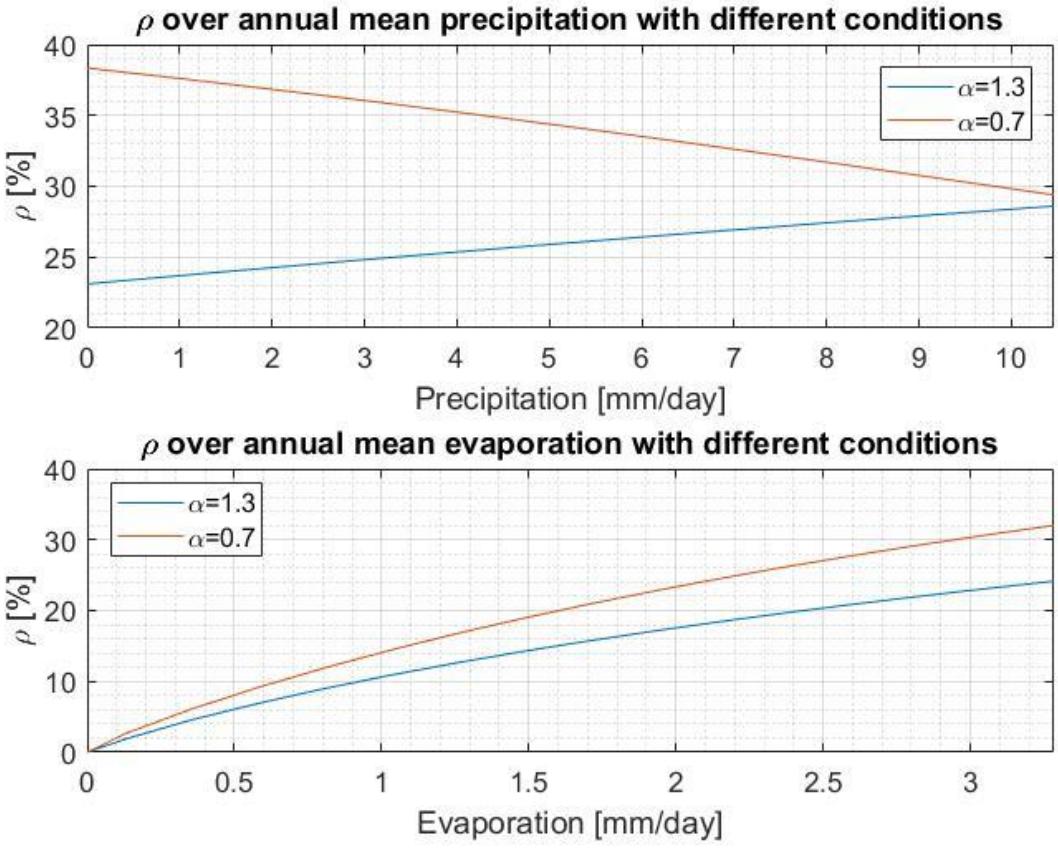

Figure 30 (A), (B). ρ over E and P under different conditions. Figure 31 (A) shows ρ over P under LED and AD conditions. Figure 31 (B) shows that E has positive contribution under any condition.

Figure 30(A) shows that precipitation has a positive contribution to ρ under AD condition. But, if the condition changes from AD to LED, the contribution of P to ρ becomes negative. AD condition means water vapors from advection source have greater chances to be condensed than those from local evaporation. And E is maintained constant in this case. Therefore, increased precipitation is identified as water vapors from advection source are condensed more frequently than those from local evaporation under AD condition. For this reason, the recycling ratio becomes decreased, based on the definition of recycling ratio. So, the simulations present well contribution of E and P to ρ for the two conditions such as LED and AD conditions. Figure 31 (B) shows positive contributions of E to the recycling ratio (ρ) under the

two conditions (LED, AD) That follows equation (16) and definition of recycling ratio. As the E increased, ratio of P from local evaporation to P from advection will be increased while the given amount of total precipitation is remained as constant amount. And while the P increases from 0 to 11 [mm/day], ρ increases from 0 to 32.02 under LED conditions when α is equal to 0.7. At the same time, ρ increases from 0 to 24.15 under AD condition when α is equal to 1.3. This shows that sensitivity of E is greater than that of P in both of conditions.

Chapter 4.2 and 4.3 show that the distribution of ρ is strongly related with topological aspect of the domain. Especially case studies in 4.3 demonstrate the effect of α on ρ and provide some clues about other possible factors to influence on ρ. This study suggests deterministic factors to the distribution as topography, direction and size of advection coupled with wind vectors. And cases of 1997 and 1998 in Figure 19, 20, extreme weather phenomenon such as El Nino, was suggested as hypothesis to determine location and distribution of ρ over the domain. But in any case, the size of α is the most influential to the size of ρ with given E and P. The most interesting part of Chapter 4 is different contributions of E and P to the recycling ratio shown in Chapter 4.4.1 and 4.4.2. The role of evaporation (E) is to add precipitation from water vapor of E (evaporation) in both of ELP, AD conditions. That can suggest another hypothesis of recycling issue. Deterministic factors to evaporation such as agricultural activities, deforestation, can change the recycling ratio and make the precipitation of the area more dependent on local evaporation or advection. So, the land use and types of land coverage would have huge impact on the recycling ratio under LED condition or α is less than one rather than AD condition or α is greater than one. Because the recycling ratio is more sensitive under LED condition, the change of E due to land use change and land cover change would influence more seriously than cases under AD conditions. Also, this result matches up with the result of Chapter 4.1. But,

precipitation (P) shows different role to the recycling ratio as mentioned before. The contribution of P to ρ varies depending on the not well-mixed conditions characterized by α.

5. Conclusion and Future Work

Precipitation recycling ratio characterizes the contribution of local evaporation to total precipitation. It is a diagnostic variable for understanding the interaction between land and atmosphere in terms of energy (evaporation) and mass balance (precipitation, evaporation). Conventional models of precipitation recycling ratio are based on well-mixed assumption that water vapors in the atmosphere from local evaporation and advection have the same probability to be condensed. This study generalizes the well-mixed assumption to formulate a new model based on not well-mixed assumption.

The new model starts from a question about how the not well-mixed conditions can be expressed and how it will work under given meteorological conditions of evaporation, precipitation, and vertically integrated precipitable water. A new parameter α was introduced to present the not-well mixed conditions. α characterizes the relative probability of water vapors from local evaporation and from advection being condensed out as precipitation. α less than one represents local evaporation dominant condition; α equal to one the well-mixed condition; α greater than one the advection dominant condition. ρ is strongly affected by α, wind velocity coupled with specific humidity, the topography of the domain, and events such as El Nino.

Among the identified factors affecting recycling ratio, α is the most influential one. E and P have different contributions based on the size of α or type of not-well mixed conditions. E always has positive contribution to ρ while the contribution of P varies with α. Under the LED condition, P has positive contribution to ρ, while it has a negative contribution to ρ under AD condition. The contributions of P to ρ is depending on the types of not -well mixed condition such as LED and AD conditions.

Recycling ratio is also dependent on topography and wind velocity vector coupled with specific humidity. Global scale events such as El Nino can be a factor to contribute the distribution of ρ. For example, El Nino brings large amount of precipitation to the Southern Brazil due to strong advection directly influencing the distribution of ρ.

Future work includes modeling recycling ratio using updated higher resolution data products, including tropical rainfall measurement mission (TRMM) and global precipitation measurement (GPM). TRMM is a research satellite covering the tropical and subtropical area including the domain of this study. GPM is an international satellite mission to provide next-generation observations of global rain and snow every three hours. The two data sets will be adopted in the future work. And global analyses with finer data sets will help to get better understanding of precipitation recycling issues and its practical aspects. Another future work is about α. So far, we do not know whether α is regional specific or dependent on physical conditions such as balances between strength of advection and that of evaporation. The future work will seek answers to these questions.

Appendix

A. Evaluation of the not-well mixed model base on Equation 13.

To evaluate equation (13), let assume a situation as there is no precipitation so the recycling ratio or ρ does not exist. If the recycling ratio at i (time) is set as ρ_i and a recycling ratio at i+1 is set as ρ_{i+1}, the ρ_{i+1} is expressed with Huen's method (references?) as below.

$$\rho_{i+1} = \rho_i + 0.5 * ((\alpha - \rho_{i+1})\frac{E_{i+1}}{w_{i+1}} + (\alpha - \rho_i)\frac{E_i}{w_i})\Delta t$$

$$\left(1 + 0.5 * \frac{E_{i+1}}{w_{i+1}}\Delta t\right)\rho_{i+1} = \rho_i + 0.5 * \alpha * \frac{E_{i+1}}{w_{i+1}}\Delta t + 0.5 * (\alpha - \rho_i)\frac{E_i}{w_i}\Delta t$$

$$\rho_{i+1} = \frac{\rho_i + 0.5 * \left(\alpha * \frac{E_{i+1}}{w_{i+1}} + (\alpha - \rho_i)\frac{E_i}{w_i}\right)\Delta t}{\left(1 + 0.5 * \frac{E_{i+1}}{w_{i+1}}\Delta t\right)}$$

For evaluation, the equation above, let assume there is no precipitation. Under the assumption and boundary condition, $\rho_1 = \frac{\rho_0 + 0.5 * \left(\alpha * \frac{E_1}{w_1} + (\alpha - \rho_0)\frac{E_0}{w_0}\right)\Delta t}{\left(1 + 0.5 * \frac{E_1}{w_1}\Delta t\right)}$ the boundary conditions are ρ_0=0, $E_0 =$ 0. But if ρ_1 is not existent, E1, w_1, $w_0$must be not applicable to the equation. That case is only possible with conditions such as non-existent E or w0 or w1 as zero. But all of the possible conditions are not possible, so the linear relation between precipitation recycling ratio and a ratio of local precipitable water to total precipitable water is not appropriate.

B. Numerical expression for the precipitation combined with power function of α

Based on Euler's method, it can be expressed as 1st order implicit solution.

$$\rho_{i+1} = \rho_i + \left[\alpha\left(\rho_i^{1-\beta} - \rho_i\right)\frac{E}{w} - \alpha\left(\rho_i^{2-\beta} - \rho_i\right)\frac{P}{w}\right]h$$

$$\rho_{i+1} = \rho_i + \frac{1}{2}\left[(\alpha - \rho_i)\frac{E_i}{w_i} + (1-\alpha)\rho_i\frac{P_i}{w_i} + (\alpha - \rho_{i+1})\frac{E_{i+1}}{w_{i+1}} + (1-\alpha)\rho_{i+1}\frac{P_{i+1}}{w_{i+1}}\right]h$$

$$\left(2 + \frac{E_{i+1}}{w_{i+1}}h - (1-\alpha)h\frac{P_{i+1}}{w_{i+1}}\right)\rho_{i+1} = 2\rho_i + \left[(\alpha - \rho_i)\frac{E_i}{w_i} + (1-\alpha)\rho_i\frac{P_i}{w_i} + \alpha\frac{E_{i+1}}{w_{i+1}}\right]h$$

$$\rho_{i+1} = \frac{2\rho_i + \left[(\alpha - \rho_i)\frac{E_i}{w_i} + (1-\alpha)\rho_i\frac{P_i}{w_i} + \alpha\frac{E_{i+1}}{w_{i+1}}\right]h}{\left(2 + \frac{E_{i+1}}{w_{i+1}}h - (1-\alpha)\frac{P_{i+1}}{w_{i+1}}h\right)}$$

With Runge Kutta Method, the equation is expressed below.

$$\frac{d\gamma(x,y,t)}{dt} = (1-\gamma)\frac{E(x,y,t)}{w(x,y,t)} - (\gamma^{\alpha} - \gamma)\frac{P(x,y,t)}{w(x,y,t)}$$

$$\gamma_{i+1}(x_{i+1}, y_{i+1}, t_{i+1}) = \gamma_i(x_i, y_i, t_i) + \frac{1}{6}(l_1 + 2l_2 + 2l_3 + l_4)h$$

$$l_1 = (1 - \gamma_i(x_i, y_i, t_i))\frac{E(x_i, y_i, t_i)}{w(x_i, y_i, t_i)} - (\gamma_i^{\alpha}(x_i, y_i, t_i) - \gamma_i(x_i, y_i, t_i))\frac{P(x_i, y_i, t_i)}{w(x_i, y_i, t_i)}$$

$$l_2 = \left[1 - \gamma_i\left(x_i + \frac{1}{2}k_1h, y_i + \frac{1}{2}j_1h, t_i + \frac{1}{2}h\right)\right]\frac{E\left(x_i + \frac{1}{2}k_1h, y_i + \frac{1}{2}j_1h, t_i + \frac{1}{2}h\right)}{w\left(x_i + \frac{1}{2}k_1h, y_i + \frac{1}{2}j_1h, t_i + \frac{1}{2}h\right)} - \left[\gamma_i^{\alpha}\left(x_i + \frac{1}{2}k_1h, y_i + \frac{1}{2}j_1h, t_i + \frac{1}{2}h\right) - \gamma_i\left(x_i + \frac{1}{2}k_1h, y_i + \frac{1}{2}j_1h, t_i + \frac{1}{2}h\right)\right]\frac{P\left(x_i + \frac{1}{2}k_1h, y_i + \frac{1}{2}j_1h, t_i + \frac{1}{2}h\right)}{w\left(x_i + \frac{1}{2}k_1h, y_i + \frac{1}{2}j_1h, t_i + \frac{1}{2}h\right)}$$

$$l_3 = \left[1 - \gamma_i\left(x_i + \frac{1}{2}k_2h, y_i + \frac{1}{2}j_2h, t_i + \frac{1}{2}h\right)\right]\frac{E\left(x_i + \frac{1}{2}k_2h, y_i + \frac{1}{2}j_2h, t_i + \frac{1}{2}h\right)}{w\left(x_i + \frac{1}{2}k_2h, y_i + \frac{1}{2}j_2h, t_i + \frac{1}{2}h\right)} - \left[\gamma_i^{\alpha}\left(x_i + \frac{1}{2}k_2h, y_i + \frac{1}{2}j_2h, t_i + \frac{1}{2}h\right) - \gamma_i\left(x_i + \frac{1}{2}k_2h, y_i + \frac{1}{2}j_2h, t_i + \frac{1}{2}h\right)\right]\frac{P\left(x_i + \frac{1}{2}k_2h, y_i + \frac{1}{2}j_2h, t_i + \frac{1}{2}h\right)}{w\left(x_i + \frac{1}{2}k_2h, y_i + \frac{1}{2}j_2h, t_i + \frac{1}{2}h\right)}$$

$$l_4 = (1 - \gamma_i(x_i + k_3h, y_i + j_3h, t_i + h))\frac{E(x_i + k_3h, y_i + j_3h, t_i + h)}{w(x_i + k_3h, y_i + j_3h, t_i + h)} - (\gamma_i^{\alpha}(x_i + k_3h, y_i + j_3h, t_i + h) - \gamma_i(x_i + k_3h, y_i + j_3h, t_i + h))\frac{P(x_i + k_3h, y_i + j_3h, t_i + h)}{w(x_i + k_3h, y_i + j_3h, t_i + h)}$$

Reference

1. Bosilovich, M. G., et al. (2003). " Numerical simulation of the large-scale North American monsoon water sources, J. Geophys. Res., **108**, 8614.

2. Brubaker, K. L., et al. (1993). "Estimation of Continental Precipitation Recycling." Journal of Climate **6**(6): 1077-1089.

3. Burde, G. I. (2006). "Bulk Recycling Models with Incomplete Vertical Mixing. Part I: Conceptual Framework and Models." Journal of Climate **19**(8): 1461-1472.

4. Burde, G. I. and A. Zangvil (2001). "The Estimation of Regional Precipitation Recycling. Part I: Review of Recycling Models." Journal of Climate **14**(12): 2497-2508.

5. Costa, M. H., et al. (2003). "Effects of large-scale changes in land cover on the discharge of the Tocantins River, Southeastern Amazonia." Journal of Hydrology **283**(1): 206-217.

6. Delaygue, G., et al. (2000). "The origin of Antarctic precipitation: a modelling approach." Tellus B **52**(1).

7. Eltahir, E. A. B. and R. L. Bras (1994). "Precipitation recycling in the Amazon basin." Quarterly Journal of the Royal Meteorological Society **120**(518): 861-880.

8. Fitzmaurice, J. A., (2007). A critical analysis of bulk precipitation recycling models. Massachusetts Institute of Technology.

9. Goessling, H. F. and C. H. Reick (2013). "On the "well-mixed" assumption and numerical D tracing of atmospheric moisture." Atmos. Chem. Phys. 13(11): 5567-5585.

10. Grimm, A. M., et al. (2000). "Climate Variability in Southern South America Associated with El Niño and La Niña Events." Journal of Climate **13**(1): 35-58.

11. Hai, H. E. and L. U. Guihua (2013). "Precipitation Recycling in Tarim River Basin." Journal of Hydrologic Engineering 18(11): 1549-1556.

12. Kalnay, E., et al. (1996). "The NCEP/NCAR 40-Year Reanalysis Project." Bulletin of the American Meteorological Society **77**(3): 437-471.

13. Kistler, R., et al. (2001). "The NCEP–NCAR 50–Year Reanalysis: Monthly Means CD–ROM and Documentation." Bulletin of the American Meteorological Society **82**(2): 247-267.

14. Koster, R. D., et al. (1993). "Continental water recycling and H218O concentrations." Geophysical Research Letters **20**(20): 2215-2218.

15. Koster, R. D., et al. (1992). "Origin of July Antarctic precipitation and its influence on deuterium content: a GCM analysis." Climate Dynamics **7**(4): 195-203.

16. Kurita, N., et al. (2004). "Modern isotope climatology of Russia: A first assessment." Journal of Geophysical Research: Atmospheres **109**: D03102

17. Lettau, H., et al. (1979). "Amazonia's Hydrologic Cycle and the Role of Atmospheric Recycling in Assessing Deforestation Effects." Monthly Weather Review **107**(3): 227-238.

18. Numaguti, A. (1999). "Origin and recycling processes of precipitating water over the Eurasian continent: Experiments using an atmospheric general circulation model." Journal of Geophysical Research: Atmospheres **104**(D2): 1957-1972.

19. Risi, C., et al. (2013). "Role of continental recycling in intraseasonal variations of continental moisture as deduced from model simulations and water vapor isotopic measurements." Water Resources Research **49**(7): 4136-4156.

20. Salati, E., et al. (1979). "Recycling of water in the Amazon Basin: An isotopic study." Water Resources Research **15**(5): 1250-1258.

21. Savenije, H. H. G. (1995). "New definitions for moisture recycling and the relationship with land-use changes in the Sahel." Journal of Hydrology **167**(1): 57-78.

22. SHUKLA, J. and Y. MINTZ (1982). "Influence of Land-Surface Evapotranspiration on the Earth's Climate." Science **215**(4539): 1498-1501.

23. Trenberth, E. K. and J. C. Guillemot (1998). "Evaluation of the atmospheric moisture and hydrological cycle in the NCEP/NCAR reanalyses." Climate Dynamics **14**(3): 213-231.

24. van der Ent, R. J., et al. (2010). "Origin and fate of atmospheric moisture over continents." Water Resources Research **46**: W09525

25. Yoshimura, K., et al. (2004). "Colored Moisture Analysis Estimates of Variations in 1998 Asian Monsoon Water Sources." Journal of the Meteorological Society of Japan. Ser. II **82**(5): 1315-1329.